

CHEMICAL AND ENERGETIC ASPECTS OF CVD DIAMOND GROWTH

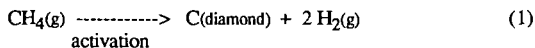
Karl E. Spear
Ceramic Science and Engineering
The Pennsylvania State University
University Park, PA 16802

INTRODUCTION

Excitement has emerged in both the scientific and industrial communities with the development of techniques for creating crystalline diamond films and coatings using low pressure gases rather than the high pressures and temperatures previously considered essential.(1) These developments have opened a new era in diamond technology and offer the potential for exploiting diamond's unique properties in applications ranging from coatings for cutting tools, to free standing windows and lense coatings for visible and infrared transmission, to thin films for high temperature, high power semiconductor devices.

Applications requiring advanced materials can uniquely utilize diamond because it (i) is the hardest known material, (ii) has the highest room temperature thermal conductivity of any material, (iii) is resistant to heat, acids, and radiation, (iv) is a good electrical insulator, but can be doped to produce either p-type or n-type semiconductors, (v) has a small dielectric constant, (vi) has a large hole mobility, and (vii) is transparent to visible and infrared radiation.(1) The high pressure-high temperature (HPHT) synthetic diamonds developed by General Electric in the 1950's (2) are now commonplace in cutting, grinding, and polishing, but many potential applications of diamond require thin films or coatings which cannot be produced from either natural or HPHT synthetic diamonds.

The diamond coating process which has generated the recent excitement utilizes temperature and pressure conditions under which graphite is clearly the stable form of carbon. However, kinetic factors allow crystalline diamond to be produced by a net chemical reaction of:



In addition to methane, a wide variety of carbon containing reactant gases can be used. The typical process consists of a reactant gas at less than atmospheric pressure which contains >95% hydrogen and is activated by passing it through a plasma or past an ~2000°C filament before contacting an 800-1000°C substrate on which the diamond is deposited.

Many questions must be answered concerning this deceptively simple looking "metastable" process before the potential of the new coating technology can be realized. Our understanding of the basic science must be extended far beyond our present knowledge, a challenge currently being met by laboratories around the world. The aim of this article is to summarize our current understanding of the chemical and energetic aspects of the growth processes for crystalline diamond.

CHEMICAL OBSERVATIONS

Many experimental observations concerning the activated vapor deposition of crystalline diamond have been made, particularly by Russian scientists Derjaguin, Fedoseev, Spitsyn, and co-workers. They have developed an extensive experimental base of chemical and kinetic information, and have proposed global kinetic theories for diamond growth based on nucleation theory, Langmuir adsorption-desorption kinetics, and equilibrium. Recent reviews in English give excellent summaries of this work.(1,3-5)

A major problem in growing high-quality diamond films is the co-deposition of graphitic-like carbon. Derjaguin and co-workers experimentally determined that the addition of excess hydrogen to the hydrocarbon precursor gas led to less graphite co-deposition with crystalline diamond, and that "activating"

the precursor gas prior to deposition increased the diamond growth rates from Å/hour to μm/hour. They activated the gas using either an electric discharge in the system, or a hot tungsten filament over which the gas flowed before encountering the lower temperature deposition region. A manifestation of the competition between the growth of diamond and graphite is the temperature dependence of the diamond growth rate which exhibits a maximum near 1000°C.

Derjaguin and Fedoseev(6) made a major breakthrough in determining that atomic hydrogen is critical to achieving appreciable growth rates for crystalline diamond, and proposed that a super-equilibrium concentration of atomic hydrogen at the growth surface is responsible for the major reduction in graphite co-deposition. They argue that atomic hydrogen behaves like a 'solvent' for graphite. Their studies of the relative etching rates of diamond and graphite showed that the removal of graphite by 'activated' hydrogen was orders of magnitude faster than diamond. Setaka(7) recently reported etching rates of graphite, glassy carbon, and diamond in a hydrogen plasma under typical diamond growth conditions. In units of mg/cm²-hr, his values are 0.13 for graphite, 0.11 for glassy carbon, and 0.006 for diamond. Saito et al.(8) also showed much greater etching rates for graphite than diamond when subjecting the materials to microwave plasmas of either hydrogen, or hydrogen-1.6%water mixtures.

Derjaguin and co-workers also observed that the nature of the precursor hydrocarbon gas had little effect on the deposition behavior. Sato et al.(9) have grown diamond from gaseous mixtures of various hydrocarbons and hydrogen by plasma-assisted deposition and found similar results. Both saturated and unsaturated hydrocarbons were used, and similar growth features were noted for all the hydrocarbons when comparisons were made as a function of the C/H ratio in the input gas. The density of nucleation and the growth rates were found to be essentially the same as those observed with the more commonly used methane. Crystalline diamond has been grown using aliphatic and aromatic hydrocarbons as well as alcohols and ketones. Small amounts of O₂ added to the precursor gas accelerates the growth rate of diamond films. Diamond can also be grown from hydrogen / hydrocarbon gas mixtures which contain larger amounts of oxygen (as in an oxygen-acetylene flame).

The relative independence of diamond growth on the nature of the input hydrocarbon species is consistent with the fact that most hydrocarbon sources tend to chemically transform to common product species (such as acetylene, one of the most stable of such gaseous products) under harsh environments such as those found in high temperature pyrolysis(10,11), combustion(12), plasmas(13), and the other typical methods used for activating precursor gases in diamond deposition. Good quality diamond films have been produced under a variety of different activation methods: microwave-, rf-, uv-, laser-, and hot-filament activated gas mixtures.(1) Approximately the same growth conditions (temperature, pressure, concentrations of precursors) are needed for crystalline diamond growth, regardless of the method of activation. The method of activation influences the rate of diamond growth, but not the general structure of the deposited crystallites.

A number of ongoing spectroscopic studies of activated methane-hydrogen gas mixtures under diamond film growth conditions indicate a predominance of acetylene and methyl radical growth species. One such study by Celii et al.(14) reported *in situ* infrared diode laser absorption spectroscopy results obtained from examinations of gas phase species present during hot-filament assisted deposition of diamond films; another by Harris et al.(15) reported mass spectra investigations in a hot-filament assisted diamond growth system as a function of filament-to-substrate distance. The initial analysis of these latter authors suggests that diamond growth comes mainly from acetylene and/or methyl radical precursors, but contributions from methane and ethylene cannot be ruled out.

ENERGETICS OF GAS-SOLID GROWTH INTERFACE

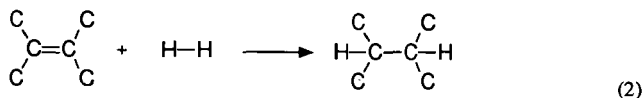
The pressure vs. temperature phase diagram for carbon given in Figure 1 clearly shows that graphite is the stable form of carbon under the conditions used for vapor depositing crystalline diamond. Why is it then possible to grow diamond at 750-1100°C and less than atmospheric pressure?

Although an established mechanistic answer is not yet available for the above question, one that is consistent with reported experimental facts can be given(16). The heart of this hypothesis on "metastable" diamond growth rests on the fact that the diamond growth process occurs at the gas-solid interface in the carbon-hydrogen system. The vapor growth process does not involve just elemental carbon, the one component which is represented on the phase diagram, but it also involves hydrogen. A diamond carbon surface saturated with sp^3 C-H bonds is more stable than a carbon surface free of hydrogen. Once a surface carbon is covered by another diamond growth layer, then that covered carbon possessing four sp^3 C-C bonds is metastable with respect to a graphitic carbon. Thus, an upper temperature limit for the vapor growth of diamond is determined by the kinetics of the diamond-to-graphite solid state transformation (and how these kinetics are influenced by structural imperfections).

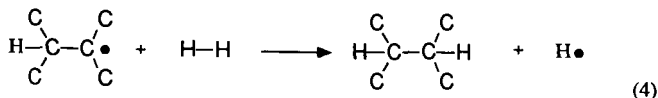
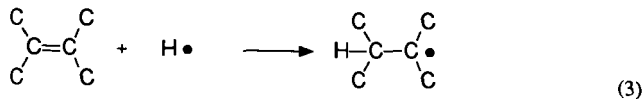
The close relationship between the diamond and graphite crystal structures is depicted in Figure 2. The puckered {111} planes of diamond are shaded to emphasize their relationship to the {001} planes of graphite. Hydrogen atoms are shown as satisfying the "dangling sp^3 bonds" of the carbons on the top diamond plane. Without the hydrogens maintaining the sp^3 character of these surface carbons, it is easy to imagine the {111} diamond planes collapsing into the more stable planar graphite structure during the growth process. In fact, in the absence of hydrogen, it is well known that the surface atoms on cleaned bulk diamond crystals will reconstruct from their bulk-related surface sites at about 900-1000°C. However, in hydrogen, the surface sp^3 bonds are satisfied by C-H bonding.(17-20)

The question then arises as to why earlier thermal CVD studies utilizing hydrogen-methane mixtures for epitaxial growth on diamond surfaces were of very limited success [see, for example, Angus et al.(21)]. The pressure-temperature-composition conditions used by these earlier researchers were quite similar to those currently used for the successful activated vapor growth of crystalline diamond, but the primary deposition product was always graphitic-like carbon in these early studies.

The net saturation of a C=C double bond with hydrogen



yields a favorable negative enthalpy change, $\Delta H^0(\text{reaction}) = -126 \text{ kJ}$. However, an activation energy to produce either a carbon or a hydrogen radical will be required to get the net reaction to proceed at a significant rate. Likely mechanistic radical reactions are



where a hydrogen radical attacks the C=C double bond to produce a carbon radical, which then reacts with a hydrogen molecule to complete the saturation and regenerate a hydrogen radical. This is in agreement with the fact that only when gas activated deposition methods were first employed in the 1970's did the growth rates of crystalline diamond become large enough to be of technological interest.

As was mentioned in the section on the chemistry of diamond growth, atomic hydrogen etches sp^2 graphitic carbon at a much higher rate than it etches sp^3 diamond carbons. Thus, the source of hydrogen

atoms can serve the dual role of hindering graphite growth as well as etching away any that does nucleate on the growing diamond surface.

The thermodynamics of the deposition process may place a lower limit on the deposition temperature for a given total pressures and gas concentration. Without some type of surface activation such as bombardment, the surface reactions for deposition may approach their thermal equilibrium limits. The fact that faceted diamond crystals are produced during deposition is a typical indication that surface mobilities are large enough for surface reactions to reach equilibrium. Which reactions reach their equilibrium limits, and which ones are kinetically limited is still an open question, but it is still of value to consider the thermodynamic limits for the deposition process.

Two plots of the output of equilibrium calculations are shown in Figure 3 to illustrate how the deposition limits depend on experimental parameters.(16) Such calculations have also be made by Bichler et al.(22) and Sommer et al.(23) The fraction of carbon deposited from methane-hydrogen mixtures is plotted versus temperature for several pressures and compositions. Two important observations can be made:

- (1) The fraction of carbon deposited changes from practically zero at lower temperatures to close to 100% over two hundred degrees.
- (2) High pressures and/or low methane concentrations increase the lower temperature limit required to obtain any deposit.

Thus, thermodynamic considerations set a lower temperature limit on diamond growth of about 400 – 600°C, depending on specific pressure–composition conditions, unless “non–equilibrium” bombardment techniques are used. These latter techniques always produce some diamond-like carbon (DLC), or similar highly defective form of carbon, along with crystalline or microcrystalline diamond.

Not shown on the above plots is the fact that the elemental gaseous carbon species of C, C₃, C₅, etc. have negligible partial pressures at about 2000°C and lower. Also, at 2000°C, a typical temperature for the filament in the hot-filament-activated systems, the quantity of atomic hydrogen in equilibrium with about 10 torr of molecular hydrogen is close to 7 at. %, an appreciable amount to interact at the 800–1000°C substrate temperature.

CONCLUDING REMARKS

Under the temperature-pressure conditions used for the growth of diamond from the vapor, graphite is clearly the most stable form of carbon. However, the energy differences between depositing diamond and graphite are quite small, so kinetic factors will determine which solid phase is deposited in the carbon-hydrogen system. Even so, energetic arguments are still important in explaining the experimental observations.

At the solid-gas interface where the diamond nucleation and growth processes are occurring, a diamond surface with hydrogens satisfying the “dangling” sp³ carbon bonds is energetically more favorable than a graphite surface. If diamond forms during deposition, and its surface is adequately saturated with sp³ C-H bonds, then graphite can subsequently form only through a solid state transformation, which is kinetically unfavorable until temperatures greater than ~1600°C are reached. If graphite forms during the deposition process, atomic hydrogen can saturate the C=C double bonds to produce a diamond surface with sp³ carbons, or it can preferentially remove the graphite through a chemical etching process. Without the presence of atomic hydrogen, the rates of saturating surface C=C bonds and the rates of graphite etching are slow compared to the solid carbon deposition, so graphitic-like carbon may dominate the process. This delicate balance between deposition rate and the concentration of atomic hydrogen has not yet been quantitatively measured.

The role of atomic hydrogen in the etching of graphitic-like carbon may be shifted to oxygen in systems containing appreciable amounts of this element, such as in the growth of diamonds from flames.

However, oxygen will probably not be important in stabilizing a diamond surface by saturating the "dangling" sp^3 carbon bonds on such a surface. The experimental and theoretical expertise which has evolved over the years in the area of combustion chemistry is clearly needed to develop quantitative models for the growth of diamond from C-H-O vapor systems.

ACKNOWLEDGMENTS

This research was sponsored by the Office of Naval Research, contracts #N00014-86-K-0283 and #N00014-86-K-0443.

REFERENCES

- (1) Karl E. Spear, *J. Am. Cer. Soc.* (review article to be published Feb. 1989)
- (2) F.P. Bundy, H.T. Hall, H.M. Strong, and R.J. Wentorf, Jr. *Nature*, **1955**, 176, 51.
- (3) D.V. Fedoseev, V.P. Varnin, and B.V. Derjaguin, "Synthesis of Diamond in Its Thermodynamic Metastability Region," *Russ. Chem. Rev.*, **1984**, 53(5), 435.
- (4) A.R. Badzian and R.C. DeVries, *Mat. Res. Bull.*, **1988**, 23, 385.
- (5) J.C. Angus and C.C. Hayman, *Science*, **1988**, 241, 913.
- (6) B.V. Derjaguin and D.V. Fedoseev, *Growth of Diamond and Graphite from the Gas Phase*, Izd. Nauka, Moscow (1977).
- (7) N. Setaka, *Chemical Vapor Deposition 1987*, Proc. Tenth Internat. Conf. on Chemical Vapor Deposition (G.W. Cullen and J. Blocher, Jr., eds.) Electrochem. Soc., Pennington, NJ, (1987), p. 1156.
- (8) Y. Saito, K. Sato, H. Tanaka, K. Fujita, and S. Matsuda, *J. Mater. Sci.*, **1988**, 23, 842.
- (9) Y. Sato, M. Kamo, and N. Setaka, *Proc. 8th Internat. Sympos. Plasma Chem.* Vol. 1 (K. Akashi and A. Kinbara, eds.), Tokyo, Aug. 31-Sept. 4, 1987, p. 2446.
- (10) R.E. Duff and S.H. Bauer, *J. Chem. Phys.*, **1962**, 36, 1754.
- (11) S.C. Khandelwal and G.B. Skinner, in *Shock Waves in Chemistry* (A. Lifshitz, ed.) Marcell Dekker, NY (1981), p. 1.
- (12) I. Glassman, *Combustion*, 2nd ed., Academic Press, NY (1987).
- (13) H.V. Boenig, Chapt. 4 in *Plasma Science and Technology*, Cornell University Press, Ithaca, NY (1982), p. 75.
- (14) F.G. Celii, P.E. Pehrsson, H.T. Wang and J.E. Butler, *Appl. Phys. Lett.*, **1988**, 52(24), 2043.
- (15) S.J. Harris, A.M. Weiner, and T.A. Perry, *Appl. Phys. Lett.*, **1988**, 53, 1605.
- (16) K.E. Spear, M. Frenklach, A. Badzian, T. Badzian, and R. Messier, *Ceram. Eng. Sci. Proc.*, **1988**, 9(9-10), 1095.
- (17) A.R. Badzian, in *Advances in X-Ray Analysis*, Vol. 31 (C.S. Barrett, J.V. Gilfrich, R. Jenkins, J.C. Russ, J.W. Richardson, and P.K. Predecki, eds.) Plenum Publishing Corp. New York (1988), p. 113.
- (18) J.M. Thomas, in *The Properties of Diamond*, (J.E. Field, ed.) Academic Press, New York, (1979), p. 211.
- (19) K.C. Pandey, *Phys. Rev.*, **1982**, B25, 4338.
- (20) B.B. Pate, *Surface Science*, **1986**, 165, 83.
- (21) J.C. Angus, H.A. Will, and W.S. Stanko, *J. Appl. Phys.*, **1968**, 39, 2915.
- (22) R. Bichler, R. Haubner, and B. Lux, *Proc. 6th European CVD Conf.*, Jerusalem (1987), p. 413.
- (23) M. Sommer, K. Mui, and F.W. Smith, presented at the *SDIO/IST - ONR Diamond Technology Initiative Symposium*, Crystal City, VA, July 12-14, 1988.

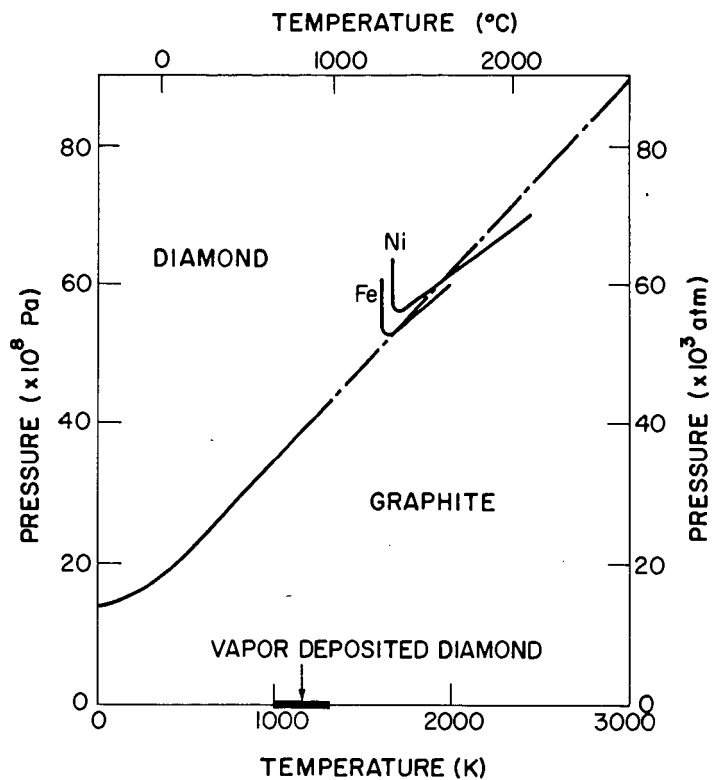
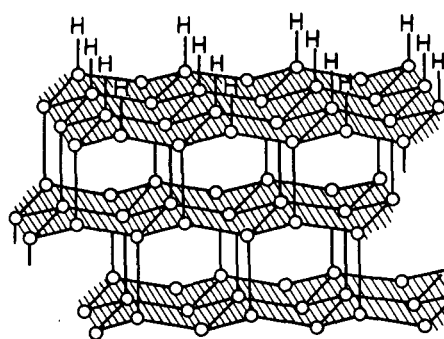
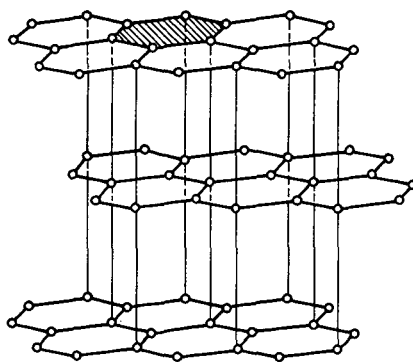


Figure 1: Pressure vs Temperature Phase Diagram for Carbon . The lines labeled with metallic elements denote the high pressure-high temperature (HPHT) conditions utilized for diamond growth using metallic solvents.



DIAMOND



GRAPHITE

Figure 2: Schematic Diagrams Showing the Similarities in the Crystal Structures of Diamond and Graphite. The hydrogen atoms bonded to the surface carbons depict their role in stabilizing the diamond surface structure.

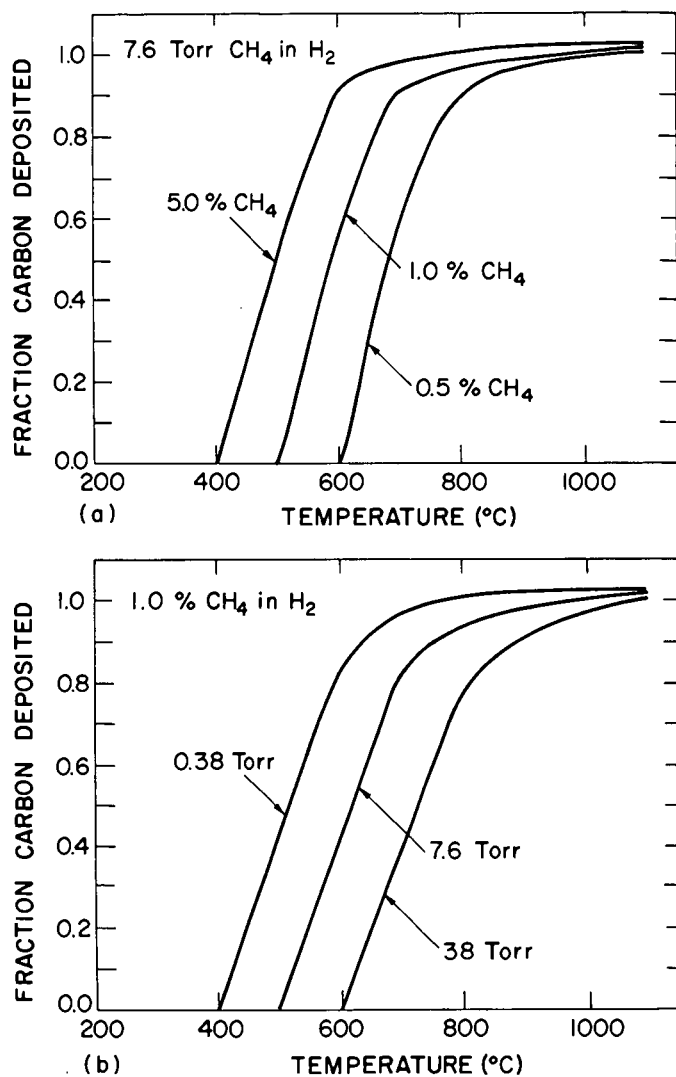


Figure 3: Equilibrium Plots of the Fraction Carbon Deposited from Methane/Hydrogen Mixtures as a Function of Temperature. (a) Constant total pressure, varying CH₄ content in reactant gas (b) Constant CH₄ content, varying total pressure.

DIAMOND SYNTHESIS IN FLAMES

L. M. Hanssen, W. A. Carrington*,
D. Oakes^A, J. E. Butler^T, and K. A. Snail
Code 6522, Optical Sciences Division
Naval Research Laboratory
Washington, D.C. 20375-5000

INTRODUCTION

The synthesis of diamond in an atmospheric pressure flame was first reported by Hirose and Kondo¹ in March, 1988. The conditions leading to diamond growth were given as an oxygen/acetylene flow ratio of 1.5/2, a substrate temperature of 1000°C, and a Si substrate positioned in the 'inner' or acetylene feather region of the flame. Slower diamond growth was also observed in a hydrogen-methane flame with a filament. More recently, Hirose and Mitsuizumi² have reported growing diamond with acetylene, ethylene, methane, propane, methanol and ethanol gases burned in air when mixed with either hydrogen or oxygen. Growth was achieved on Si, SiC, Al₂O₃, W, WC, and Mo substrates in an oxygen-acetylene flame, and maximum growth rates of 200 µm/hr for particles² and 100-150 µm/hr for films³ were reported. The effects of varying key parameters on diamond growth were not discussed in these reports.

In the U.S., Hanssen et al.⁴ studied the effect of substrate position, fuel/oxidizer gas flow ratio, and substrate temperature on diamond growth in an premixed oxygen-acetylene flame, and observed growth on Si(100), Si(111), BN, Mo(100), Nb(100), TiC(100), Ta and Cu. Carrington et al.⁵ reported diamond growth on Si(100) in an oxygen-ethylene flame. Yarbrough⁶ confirmed the growth of diamond in an oxygen-acetylene flame at atmospheric pressure. Snail et al.⁷ observed diamond growth in an oxygen-ethane flame, studied the uniformity of diamond crystallite growth as a function of position in an oxygen-acetylene flame, and reported that adding hydrogen to an oxygen-acetylene flame increased the ratio of the (diamond / amorphous carbon) Raman peaks. Recently Yarbrough observed diamond growth in a low pressure (25 torr) oxygen-acetylene flame.⁸

The next section of this paper discusses the experimental apparatus used at the Naval Research Laboratory (NRL) to study diamond synthesis in flames. Following that, a partial review of the results obtained at NRL on the flame synthesis of diamond is given. The results of several other studies currently in progress will be presented at the meeting.

EXPERIMENTAL SETUP

An oxygen-acetylene brazing torch (see Fig. 1) fitted with a .89 mm orifice tip was used to deposit diamond crystallites and films. The torch was mounted on an xyz translation stage and the gas flow rates were adjusted with mass flow controllers. Substrates were mounted on a water cooled copper block and a two color near infrared pyrometer was used to monitor the peak substrate temperature from 650°C to 1200°C. A more detailed description of this setup can be found in Ref. 4.

Most of the depositions reported on in this paper were grown on Si(100) substrates which were prepared by scratching with 5-6 micron diamond paste, and ultrasonic cleaning in acetone and methanol. A typical deposition lasted for 10-15 minutes. During depositions the torch was operated in a fuel rich mode and the substrates were positioned in the first diffusion flame (or 'acetylene feather') beyond the premixed flame front.

The substrate temperature distribution was monitored during depositions with a thermal (8-12 μm) imaging camera having a spatial resolution on the substrate of $\sim 1/3$ mm (3 mrad). During several long (2-4 hours) depositions, a zoom microscope (10-70x) with a video camera attachment was used to record the changes in crystallite morphology with time. Square faced (100) diamond crystallites with up to 350 micron sized edges have been grown during these longer depositions, using an oxygen-acetylene flame.

RESULTS AND DISCUSSION

In the first subsection of this section, the oxygen/acetylene flow ratios and substrate temperatures which lead to the growth of faceted diamond crystallites, micro-crystalline graphite and amorphous carbon (a-C) are reviewed. Adding hydrogen to an oxygen-acetylene flame is then discussed in terms of its effect on the a-C contributions to the crystallite's Raman spectra and the crystallite morphology. Finally, the variation in diamond crystallite growth with position in a premixed oxygen-acetylene flame is analyzed.

Process parameters - material property relationships

A detailed mapping of the type of material deposited versus the substrate temperature and fuel/oxidizer flow ratio has been performed for an oxygen-acetylene flame. The ($\text{O}_2/\text{C}_2\text{H}_2$) flow ratio, R, was varied from 0.8 to 1.5; this corresponds to a range of equivalence ratios⁹ of 3.13 - 1.67, respectively. The total gas flow rate was ~ 2.3 slm and the substrate was positioned 1-2 mm below the inner flame tip. The substrate temperature was varied from 650°C to 1200°C. The deposited material was analyzed with an optical microscope, a field emission scanning electron microscope (SEM), and also by x-ray diffraction (XRD) and Raman spectroscopy. Raman spectra were taken with a 5145 Å laser excitation and ~ 30 mm spot size. The Raman data discussed in the next two subsections were taken with ~ 1 mm spot size using a micro-Raman accessory.

As in the case of the low pressure CVD processes, well faceted crystallite growth occurs when the substrate is near 900°C. For the torch nozzle and total flow rates used, these studies indicate that for flow ratios less than 0.9, ball-like structures (see Fig. 2a, Ref. 4) grow at all substrate temperatures. For values of R between 0.9 and 1.2, well faceted crystallites grow (see Fig 2b, Ref. 4). The temperature range for which crystallite growth occurs expands from near 900°C at R = 0.9 to 650°C - 1050°C at R = 1.2. Above and below this temperature range, ball-like structure growth occurs. For R greater than 1.15, the growth rate decreases rapidly with increasing values of R so that at R = 1.2 the growth rate is very low and at 1.3 and 1.4 growth does not occur.

The variation of material morphology with substrate temperature and oxygen/acetylene ratio encompasses three distinct regions corresponding to the growth of faceted crystallites and ball-like structures, and no growth. The boundary between the ball-like structure and crystallite regions exhibits a gradual transition in particle morphology from faceted crystallites to ball-like particles. For an example of a transitional structure see Fig. 2d of Ref. 4. The diamond Raman peak at 1332 cm^{-1} is seen in the spectra of some ball-like structures and indicates that the ball-like structures can contain diamond. This suggests that measurements of the growth rates of different materials (diamond, graphite, a-C) versus the substrate temperature and oxygen/acetylene flow ratio are needed. The Raman spectra of both ball-like structures and faceted crystallites grown in an oxygen-ethylene flame also exhibited coexisting peaks due to different forms of carbon⁵.

The ball-like structures grown with R > 0.9 at substrate temperatures above those delineating the ball-crystallite boundary exhibited strong Raman peaks at 1355 cm^{-1} and 1575 cm^{-1} associated with micro-crystalline and crystalline graphite, respectively¹⁰. These peaks were also observed for ball-like structures grown at R < 0.9. Ball-like structures grown with R > 0.9 at substrate temperatures below those delineating the crystallite-ball boundary exhibited a high fluorescence background. This suggests that the region of ball-like growth may have to be further subdivided.

Hydrogen-oxygen-acetylene flames

The effect on diamond growth of adding hydrogen to an oxygen-acetylene flame was studied for two cases: first, with the $(\text{O}_2/\text{C}_2\text{H}_2)$ flow ratio fixed at 1.12, and hydrogen added to the flame, and second, with the $[\text{O}_2/(\text{C}_2\text{H}_2 + \text{H}_2)]$ flow ratio fixed at 1.12, and hydrogen substituted for acetylene. In both cases the oxygen flow rate was fixed at 1.7 slm. The total flow rate for the hydrogen addition study ranged from 3.2 slm to 4.0 slm. In the case where the $(\text{O}_2/\text{C}_2\text{H}_2)$ flow ratio was fixed, hydrogen was added so that the $(\text{H}_2/\text{C}_2\text{H}_2)$ flow ratio equalled 0.0-0.50. Most samples had an annular region of heavy crystallite nucleation; Raman spectra were taken at the inner and outer edges of the annuli, and growth center of each sample.

The ratio of the diamond to the amorphous carbon Raman peaks (R_{DC}) of individual crystallites is plotted in Figure 2 versus the $(\text{H}_2/\text{C}_2\text{H}_2)$ flow ratio for the three different positions on the samples. The R_{DC} ratio is essentially constant for crystallites located in the same local region of the sample. These results show a nearly linear increase in R_{DC} with increasing hydrogen flow rate, although the diamond growth rate decreased significantly as the $(\text{H}_2/\text{C}_2\text{H}_2)$ flow ratio exceeded 0.25. For a $(\text{H}_2/\text{C}_2\text{H}_2)$ flow ratio equal to 0.45, no growth is observed. When the $[\text{O}_2/(\text{H}_2 + \text{C}_2\text{H}_2)]$ flow ratio is fixed, substituting hydrogen for acetylene leads to an increase in R_{DC} for $(\text{H}_2/\text{C}_2\text{H}_2)$ flow ratios up to 0.02. No diamond growth is observed for $(\text{H}_2/\text{C}_2\text{H}_2)$ flow ratios equal to or greater than 5/95. This data suggests that oxygen is preferentially burning with acetylene, rather than hydrogen.

Variation of growth with position in flame

The nucleation density of crystallites deposited in an oxygen-acetylene flame was frequently higher within an annular region, and lower in other regions on the substrate. The causes of this nonuniform growth include both temperature inhomogeneities and species concentration variations. A thermal (8-12 μm) imaging camera having a spatial resolution on the substrate of $\sim 1/3$ mm (3 mrad) was used to measure substrate temperature profiles. During a typical deposition on a Si substrate in an oxygen-acetylene flame the substrate temperature profile exhibited large decrease with increasing distance from the center of the growth. For a substrate to flame front distance (D) of 4.5 mm, the temperature decrease observed from the center to edge of the diamond growth region was approximately 250°C.

The variation in diamond growth with position in the acetylene diffusion flame was studied with an oxygen flow rate of 1.7 slm and an acetylene flow rate of 1.5 slm, and is illustrated in Figure 3. When the distance (D) from the substrate to the oxygen-acetylene flame front was 3.0-4.5 (± 0.5) mm, the resulting nucleation density of diamond crystallites was low directly beneath the flame axis and significantly higher within an annulus centered on the flame axis. The outer edge of this annulus occurred where the edge of the acetylene diffusion flame intersected the substrate. As D was increased to 7.5 mm, the nucleation density increased on the region of the substrate directly under the flame axis and the annular pattern of crystallites disappeared. Growth areal density was estimated by counting crystallites in 3600 mm^2 areas using an 800X optical microscope. A weighting factor was assigned for crystallites less than 50% of the mean size in a region; the typical crystallite size ranged from 1-11 microns.

An SEM and micro-Raman study of the spatial variation of diamond crystallite quality was performed on a sample grown in an oxygen-acetylene-hydrogen flame. For this sample, the $(\text{O}_2/\text{C}_2\text{H}_2)$ flow ratio was equal to 1.12, the $(\text{H}_2/\text{C}_2\text{H}_2)$ flow ratio was set at 0.10, and the peak substrate temperature ranged from 910-960°C. The substrate was positioned 4.5 mm below the premixed flame front. Individual crystallites showed a significant decrease in the ratio (R_{DC}) of the 1332 cm^{-1} diamond Raman peak to the 1510 cm^{-1} amorphous carbon peak with increasing distance from the growth center. This variation is exhibited in Figure 4. Crystallites outside of the annular region (extending from 0.7-2.7 mm) exhibited a small increase in R_{DC} compared to those in the annulus. Electron and optical microscope analyses showed a correlation of the decrease of R_{DC} across the annular growth region with the degree of secondary growth observed on the diamond crystallite faces. Significant secondary growth was observed on crystallites in the annular growth region while 'cleaner' better formed crystallites were observed inside and outside of the annulus.

The Raman spectra of all crystallites exhibited a fluorescent background signal level which increased with the wavelength shift up to 1650 cm^{-1} , which was the limit of the measurements; this background level increased as the crystallites' distance from the growth center increased.

CONCLUSIONS AND FUTURE DIRECTIONS

These results demonstrate that diamond can be grown at atmospheric pressure in premixed oxygen-hydrocarbon flames on a variety of substrates. Growth in oxygen-acetylene flames occurs throughout the first diffusion flame beyond the premixed flame front, for acetylene rich flames. The type of material grown (diamond, graphite, a-C) in an oxygen-acetylene flame depends on the substrate temperature and oxygen/acetylene flow ratio. The ranges of the parameters found to lead to diamond crystallite growth are: 1) substrate temperatures, $T = 650$ to 1050°C , and 2) gas flow ratios, $R = 0.9$ to 1.2 for a total flow rate of ~ 2 - 3 slm (the appropriate flow rate is strongly dependent on the nozzle used). The "cleanest" crystallites were grown at $T = 950^\circ\text{C}$, and $R = 1.13$.

The addition of hydrogen to an oxygen-acetylene flame produces significant improvements in the diamond to amorphous carbon Raman peak ratio of the deposited crystallites. For an initial ($\text{O}_2/\text{C}_2\text{H}_2$) flow ratio of 1.12 , a significant decrease in crystallite growth rate occurs for ($\text{H}_2/\text{C}_2\text{H}_2$) flow ratios greater than 0.24 when hydrogen is added to the flame, and 0.02 when hydrogen is substituted for acetylene. For flames from a single orifice, the diamond crystallite growth density and quality can vary significantly with the position of the substrate in the flame. These variations are probably caused by variations in chemical species, which are known to vary significantly with position in 2d flames.

Several techniques for controlling and reducing the nonuniformities in the substrate temperature are currently under investigation. These include a mount with both heating and cooling capabilities, and using liquid metals to improve the thermal contact between the substrate and the mount. A microtube flat flame burner is currently being fabricated¹¹. This burner is expected to produce flame temperatures that are uniform to $\pm 50^\circ\text{C}$ over a 1 cm diameter disk. Several other 2d and 1d burner designs are also being studied. The nonuniform flame structure associated with single orifice flames offers an opportunity to identify the chemical species responsible for diamond growth.

* Dept. of Electrical Engineering, Thornton Hall, University of Virginia, Charlottesville, VA. 22906

[^] Office of Naval Technology Postdoctoral Fellow

[†] Chemistry Division, Code 6174, Naval Research Laboratory, Washington, DC 20375-5000

¹Y. Hirose and N. Kondo, Program and Book of Abstracts, Japan Applied Physics Spring 1988 meeting, March 29, 1988, p. 434

²Y. Hirose and M. Mitsuizumi, New Diamond 4, 34 (1988).

³Y. Hirose, "Synthesis of diamond using combustion flame in the atmosphere", Program and Abstracts Book, 1st Intl. Conf. on New Diamond Science and Tech., Oct. 24-26, 1988 (Tokyo), p. 38.

⁴L. M. Hanssen, W. A. Carrington, J. E. Butler and K. A. Snail, "Diamond synthesis using an oxygen-acetylene torch", to be published in Matls. Ltrs., Dec. 1988 or Jan. 1989.

⁵W. A. Carrington, L. M. Hanssen, K. A. Snail, D. B. Oakes, and J. E. Butler, "Diamond growth in $\text{O}_2 + \text{C}_2\text{H}_4$ and $\text{O}_2 + \text{C}_2\text{H}_2$ flames", accepted for publication in Metal. Trans. A, Sept., 1988.

⁶W. Yarbrough, presentation at the Conf. on High Performance Inorganic Thin Film Coatings, Gorham Inst. for Adv. Matls., Monterey Beach, Monterey, CA., (Oct. 1988).

⁷K. A. Snail, L. M. Hanssen, W. A. Carrington, D. B. Oakes, and J. E. Butler, "Diamond growth in combustion flames", Program and Abstracts Book, 1st Intl. Conf. on New Diamond Science and Tech., Oct. 24-26, 1988 (Tokyo), p. 142.

⁸Personal communication with W. Yarbrough, December 1988.

⁹The equivalence ratio is defined as the actual fuel:oxidizer ratio divided by the fuel:oxidizer ratio corresponding to complete combustion to carbon dioxide and water.

¹⁰F. Tuinstra and J. L. Koenig, J. Chem. Phys. **53**, 1126 (1970).

¹¹Research Technologies, P.O. Box 384, Pleasanton, CA. 94566

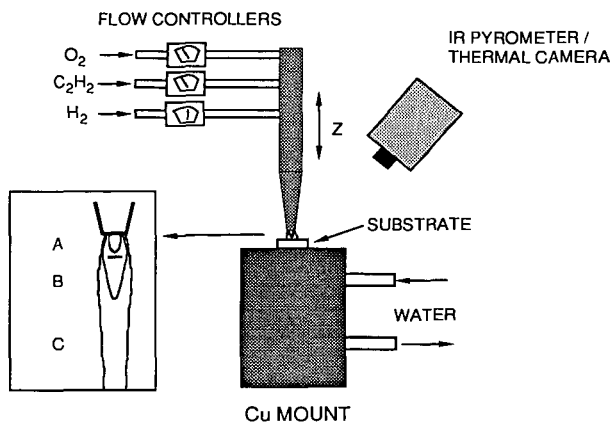


Figure 1: Schematic of the oxy-acetylene torch deposition experiment. The inset is an expanded view of the oxygen-acetylene flame. The three regions described in the text are: A) the inner cone, B) the acetylene feather, and C) the outer flame. For diamond growth, the substrate is positioned inside the acetylene feather region.

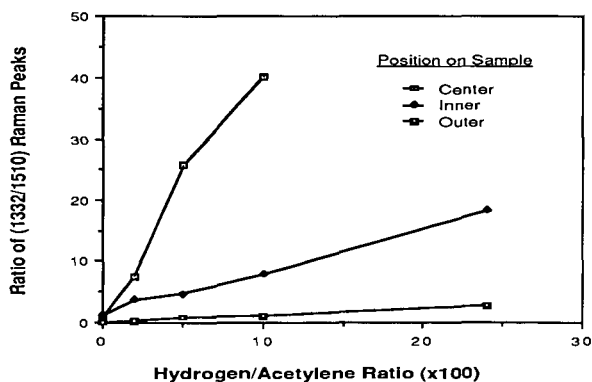


Figure 2: Ratio of the diamond Raman peak (1332 cm^{-1}) to the amorphous carbon peak (1510 cm^{-1}), for different hydrogen flow rates added to an oxygen-acetylene flame with $R = 1.12$. Data for the growth center of the sample, and the inner and outer edges of the growth annulus are shown. Note the monotonic increase in crystal quality with increasing hydrogen flow rate.

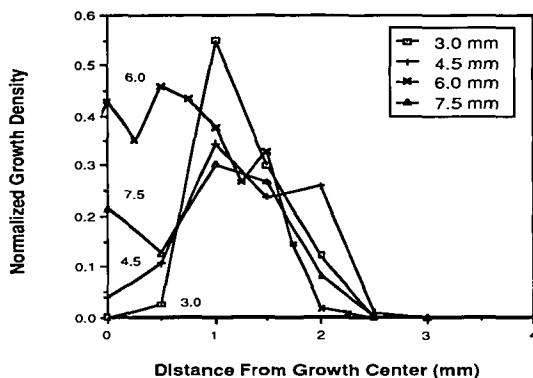


Figure 3: Normalized diamond growth density versus position on the substrate, for different flame-substrate separations (D) and the growth conditions described in the text. Note the transition from annular growth patterns to disk type patterns with increasing D.

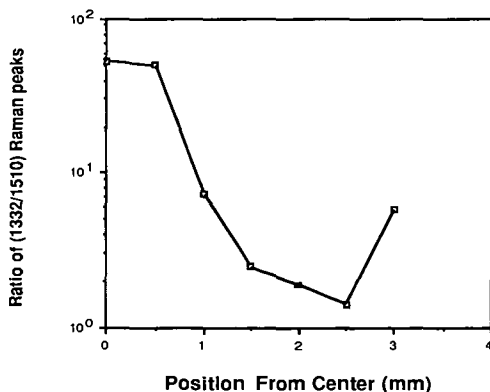


Figure 4. Ratio of the diamond Raman peak (1332 cm^{-1}) to the amorphous carbon peak (1510 cm^{-1}), versus radial distance on the substrate for the conditions described in the text. The increase at large distances is associated with positions outside of the annular growth region. SEM analysis has correlated this increase with a decrease in secondary growth on the crystallite faces.

KINETICS OF METHANE PYROLYSIS IN HOT-FILAMENT REACTOR: EFFECT OF HYDROGEN

Michael Frenklach

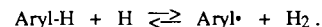
Fuel Science Program
Department of Materials Science and Engineering
The Pennsylvania State University
University Park, PA 16802

INTRODUCTION

A major breakthrough in low-pressure diamond deposition technology, that has lead to micron-a-minute growth rates, began with the addition of molecular hydrogen to the reactive hydrocarbon mixtures [1-7]. Several factors have been suggested to explain the effect of the hydrogen dilution. First, and the most important one, is the preferential etching of graphite over diamond by hydrogen atoms [1,3,4,7-10]. This theory assumes that graphite and diamond are formed simultaneously but graphite (or, more generally, graphitic phase) is destroyed by reactions with H atoms whereas diamond is not, or at least not to the same extent. Deryagin and co-workers [1,3,4,8] argued that hydrogen atoms should be in a superequilibrium state for a successful growth of diamond. The requirement of the H superequilibrium (as opposite to just a high concentration of hydrogen atoms, which, for example, can be in partial equilibrium with H₂) was rationalized by Frenklach and Spear [11] suggesting that a reversible H-atom abstraction reaction is the rate limiting step of the diamond surface growth. In a following work, using quantum mechanical methods, Huang *et al.* [12] computed that this reaction has a substantial energy barrier whereas subsequent steps of the diamond growth reaction sequence, acetylene addition to the surface radicals, have no energy barriers at all.

The second most frequently discussed [3,4,7] effect of hydrogen is to satisfy the dangling bonds of surface carbon atoms, thus keeping them in the *sp*³ configuration and preventing the diamond surface from reconstruction into graphitic *sp*² (or carbynic *sp*) structures. Other possible roles of atomic hydrogen suggested are: to promote the production of acetylene, which was proposed to be the main monomer for diamond growth, in the gas phase [11]; to promote the *sp*³ configuration of the gaseous radical precursors and surface clusters [13]; and to remove oxygen chemisorbed on the substrate [13].

The hydrogen effect was also attributed to the molecular hydrogen. Fedoseev *et al.* [3] suggested that "the addition of hydrogen to the initial hydrocarbon lowers its rate of decomposition, and therefore also the rate of formation of the solid phase." A recent computational study [14] examining the formation of polycyclic aromatic hydrocarbons (PAHs) in carbon-rich circumstellar envelopes revealed that the formation of aromatic structures, thought to be the precursors of carbonaceous solid phases [15-17], is entirely suppressed in the atmosphere of H₂ at high temperatures — temperatures that otherwise exhibit high growth rates of soot (and other forms of solid-phase carbon [18]) in fossil fuel air combustion [15] and argon-diluted pyrolysis [19]. The suppression phenomenon is explained [20-22] by the increase in the rate of the reverse direction of the abstraction reactions



It is predicted [14,22] that at lower temperatures this reaction is no longer rate-limiting and PAH growth is controlled by the rate of acetylene additions to aryl radicals. Under these conditions polycyclic aromatic hydrocarbons and solid carbon phases begin to appear.

There is an analogy between the conditions of PAH and carbon grain formation in circumstellar envelopes of carbon-rich stars [14,16,17] and CVD diamond deposition in hot-filament [23-25] and plasma-assisted [6,26] CVD reactors. In both processes the reaction takes place in hydrogen atmosphere; it is initiated by an intensive flux of energy, thermal or plasma; the reaction develops under the decrease in gas temperature; and the formation of the high molecular weight products, PAHs or diamond, occur at about the same temperatures, 800 – 1000 °C. The above theoretical considerations suggest that this analogy is not circumstantial. The results of the present computational study, aimed at the analysis of the effect of hydrogen on gaseous species under the conditions of diamond formation, demonstrate the similarity in gas-phase chemistry of the two processes, and suggest that the suppression of PAH production by molecular hydrogen plays the key role in diamond growth.

COMPUTATIONAL MODEL

The model assumed for simulation of the gas-phase chemistry is a constant pressure, constant flow rate plug-flow reactor with an imposed temperature profile. This choice is based on the following considerations. First, diamond deposition characteristics obtained in experimental reactors of different geometries and energy sources are very similar [6] and, hence, it is more logical to begin modeling the process with a simplest case, hot-filament reactor, where gas activation can be assumed to be thermal. It will be argued elsewhere that the results obtained with this assumption are also applicable to plasma-assisted CVD reactors. Second, the idealization of the gas flow is a practical necessity as neither flow characteristics, which are required for development of the gas-dynamic model, nor species profiles, that can be used to test the model predictions, have been established experimentally. Finally, and most importantly, the objective of the present simulations is to study *qualitative* trends in the computed chemical species profiles, for which the numerical accuracy of the results is not critical.

The chemical reaction mechanism used here is based on the mechanism developed for the study of PAH production in carbon-rich circumstellar envelopes [14]. It is applicable to wide ranges of temperatures, 700 – 3000 K, and pressures, up to 10^{-10} atm. The latter is compiled of 112 reactions and 39 species that describe, beginning with acetylene, the formation of benzene and its further growth to an infinitely large sized PAHs; this mechanism was adopted here without change. The 112 reactions of this mechanism were augmented with 19 reactions (adding 6 new species) describing the initial stages of methane pyrolysis: formation of CH_3 and CH_2 radicals and their subsequent reactions producing C_2H_6 , C_2H_5 , C_2H_4 and C_2H_3 , the last two being the precursors of C_2H_2 . The added reaction subset, along with the associated rate parameters, will be reported elsewhere.

The initial conditions for the "reference" case were assumed based on recent experiments of Harris *et al.* [25]: 0.3% CH_4 – H_2 mixture, pressure 20 torr, and the initial (inlet) reaction temperature 2600 K, which decreases linearly in time with the rate of 1400 K/s. Such a cooling rate means that the gas reaches the temperature of diamond deposition, ~ 1000 °C [26], within about 1 second. The computer simulations were carried until the temperature dropped to about 650 °C, well below the deposition conditions. The numerical integration of the differential equations describing the time-dependent species concentrations were performed with a constant-pressure kinetic code on a IBM 370–3090 computer at the Pennsylvania State University Computer Center using the LSODE integrator of Hindmarsh [27]. The relative error (parameter RTOL) was kept at 1×10^{-4} and the absolute error (parameter ATOL) was set well below the concentration of the principal PAH species.

RESULTS AND DISCUSSION

The concentration profiles of major species computed for the "reference" case are similar to those obtained in constant-temperature computations of Harris *et al.* [25] and in plasma simulations of

Kline and co-workers [28]. These results indicate that C_2H_2 is the major hydrocarbon species at the temperatures of diamond deposition. However, if the reaction time scale is decreased from 1 to 1×10^{-3} s (i.e., the temperature rate is changed from 1.4×10^3 K/s to 1.4×10^6 K/s), CH_4 and CH_3 become the predominant species. The residence times on the order of 1 ms have been reported by Yarbrough and Roy [23]. These authors modified the hot-filament reactor replacing the filament by bringing the gas to the substrate surface through a small-diameter tantalum tube which is heated by a surrounding wire coil to the hot-filament temperatures. Under such conditions the reaction mixture remains in contact with the hot tube for a relatively long period of time, on the order of milliseconds. As a result, the methane pyrolysis and hydrogen decomposition are accelerated by heterogeneous processes on the surface of the tube and the equilibrium between H and H_2 is likely to establish before the gas leaves the tube. A gas-phase kinetic simulation with the "reference" case but assuming the initial concentration of hydrogen atoms to be $[H]_{t=0} = ([H_2]/K_h)^{1/2}$, where K_h is the equilibrium constant of reaction $H + H = H_2$, indicated that the concentration of C_2H_2 reaches and supercedes that of CH_3 at about 100 μ s. Thus, we conclude that under thermal activation of the gas phase acetylene should be the predominant hydrocarbon species at the conditions of diamond deposition, as initially suggested by Frenklach and Spear [11] and verified in recent optical [24] and mass-spectrometric [25] measurements.

To investigate the effect of hydrogen addition, a computer simulation was performed similar to the "reference" case but with argon instead of hydrogen as diluent. The numerical results obtained in these two cases are compared in Figs. 1 through 4. The H concentration is larger by about an order of magnitude in the H_2 environment compared to that in the case of Ar (Fig. 1), which may support the H atom etching theory. The same information displayed in the form of H superequilibrium, defined as

$$f = \frac{[H]}{[H]_{eq}} = \frac{[H]}{[H_2]/K_h},$$

shows that practically the same values of f are computed in the both cases. This result indicates that the H supersaturation itself is not a critical parameter. This is understandable since the f values are extremely large ($\sim 10^7$ at 1000 °C), so that the kinetics of H atom reactions (e.g., etching) or of the following steps (e.g., acetylene addition) rather than their thermodynamics should be the controlling factors [22].

The concentration of CH_3 is computed to be significantly larger in H_2 than in Ar (Fig. 2), whereas the concentration of C_2H_2 is practically the same in the both cases (Fig. 3). At first glance, these results may support the proposal of Tsuda *et al.* [29] that CH_3 and not C_2H_2 is the main "building block" for diamond film growth. Further computational tests, that will be discussed elsewhere, clarify this point. Now it is pertinent to note that since acetylene is the main reaction product of methane pyrolysis, the proximity in C_2H_2 profiles computed in H_2 and Ar environments (Fig. 3) demonstrates that the abundance of H_2 does not lower the rate of methane decomposition. However, as seen in Fig. 4, the presence of H_2 does pronouncedly suppresses the production of aromatic hydrocarbons. It is this suppression phenomenon that is proposed here to play the critical role in the hydrogen effect on diamond growth. Aromatic species formed in the gas phase condense on the (diamond) surface, i.e., collide with the surface and held there by van der Waals forces. Their further growth leads to the formation of graphitic layers, which competes with and thus prevents the growth of diamond.

ACKNOWLEDGEMENT

The work was supported in part by the Office of Naval Research, Contracts No. N00014-86-K-0283 and N00014-86-K-0443.

REFERENCES

1. B. V. Spitsyn, L. L. Bouilov, B. V. Derjaguin, *J. Crystal Growth* **52**, 219 (1981).
2. S. Matsumoto, Y. Sato, M. Kamo, and N. Setaka, *Jpn. J. Appl. Phys.* **21**, L183 (1982).
3. D. V. Fedoseev, V. P. Varnin, and B. V. Deryagin, *Russ. Chem. Rev.* **53**, 435 (1984).
4. D. V. Fedoseev, B. V. Deryagin, I. G. Varshavskaya, and A. S. Semenova-Tyan-Shanskaya, *Crystallization of Diamond* (Nauka, Moscow, 1984, in Russian).
5. R. C. DeVries, *Ann. Rev. Mater. Sci.* **150**, 161 (1987).
6. R. Messier, A. R. Badzian, T. Badzian, K. E. Spear, P. Bachmann, and R. Roy, *Thin Solid Films*, **153**, 1 (1987).
7. J. H. Angus and C. C. Hayman, *Science* **241**, 913 (1988).
8. B. V. Spitsyn and L. L. Bouilov, in *Extended Abstracts. Diamond and Diamond-Like Materials Synthesis*, edited by G. H. Johnson, A. R. Badzian, and M. W. Geis (Materials Research Society, Pittsburgh, 1988), p. 3.
9. J. C. Angus, H. A. Will, and W. S. Stanko, *J. Appl. Phys.* **39**, 2915 (1968).
10. S. P. Chauhan, J. C. Angus, and N. C. Gardner, *J. Appl. Phys.* **47**, 4746 (1976).
11. M. Frenklach and K. E. Spear, *J. Mater. Res.* **3**, 133 (1988).
12. D. Huang, M. Frenklach, and M. Maroncelli, *J. Phys. Chem.* **92**, 6379 (1988).
13. E. S. Machlin, *J. Mater. Res.* **3**, 958 (1988).
14. M. Frenklach and E. D. Feigelson, *Astrophys. J.*, in press.
15. B. S. Haynes and H. Gg. Wagner, *Prog. Energy Combust. Sci.* **7**, 229 (1981).
16. M. Frenklach, M., in *Carbon in the Galaxy: Studies from Earth and Space*, edited by J. Tarter (NASA CP, 1988) in press.
17. A. G. Tielens, in *Carbon in the Galaxy: Studies from Earth and Space*, edited by J. Tarter (NASA CP, 1988) in press.
18. M. Frenklach, J. P. Hsu, D. L. Miller, and R. A. Matula, *Combust. Flame* **64**, 141 (1986).
19. M. Frenklach, S. Taki, M. B. Durgaprasad, and R. A. Matula, *Combust. Flame* **54**, 81 (1983).
20. M. Frenklach, D. W. Clary, W. C. Gardiner, Jr., S. E. Stein, *Twentieth Symposium (International) on Combustion* (The Combustion Institute, Pittsburgh, 1985), p. 887.
21. M. Frenklach, T. Yuan, and M. K. Ramachandra, *Energy & Fuels* **2**, 462 (1988).
22. M. Frenklach, *Twenty-Second Symposium (International) on Combustion* (The Combustion Institute, Pittsburgh, 1989), in press.
23. W. A. Yarbrough and R. Roy, in *Extended Abstracts. Diamond and Diamond-Like Materials Synthesis*, edited by G. H. Johnson, A. R. Badzian, and M. W. Geis (Materials Research Society, Pittsburgh, 1988), p. 33.
24. F. G. Celii, P. E. Pehrsson, H. T. Wang, and J. E. Butler, *Appl. Phys. Lett.* **52**, 2045 (1988).
25. S. J. Harris, A. M. Weiner, and T. A. Perry, *Appl. Phys. Lett.* **53**, 1605 (1988).
26. A. R. Badzian and T. Badzian, in *Extended Abstracts. Diamond and Diamond-Like Materials Synthesis*, edited by G. H. Johnson, A. R. Badzian, and M. W. Geis (Materials Research Society, Pittsburgh, 1988), p. 27.
27. A. C. Hindmarsh, "Towards a Systematic Collection of ODE Solvers," 10th IMACS World Congress on Systems Simulation and Scientific Computation (Montreal, 1982); also Lawrence Livermore Laboratory Preprint No. UCRL-87465, March 1982.
28. L. E. Kline, W. D. Partlow, and W. E. Bies, *Proc. Electrochem. Soc. Symp. on Plasma Processing* (ECS, Pennington, N.J., 1987); also *J. Appl. Phys.* (1988), to appear.
29. M. Tsuda, M. Nakajima, M., and S. Oikawa, S., *Jpn. J. Appl. Phys.* **108**, 5780 (1987).

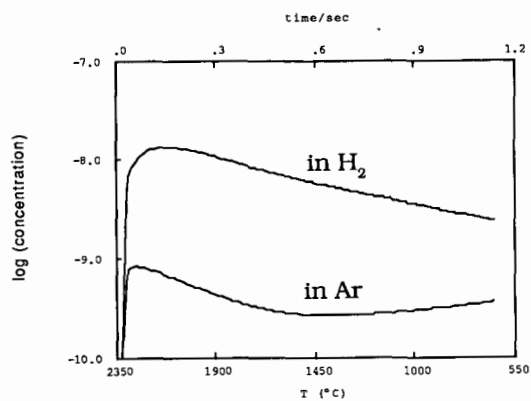


Fig. 1. Concentration of H

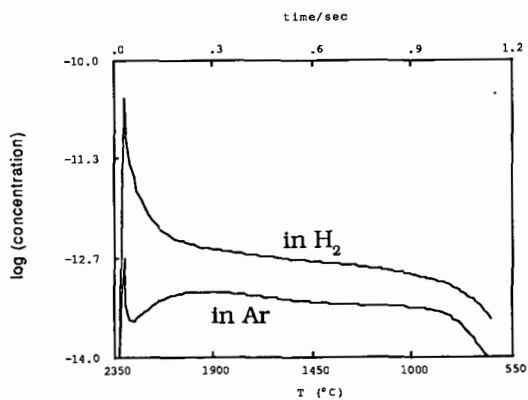


Fig. 2. Concentration of CH₃

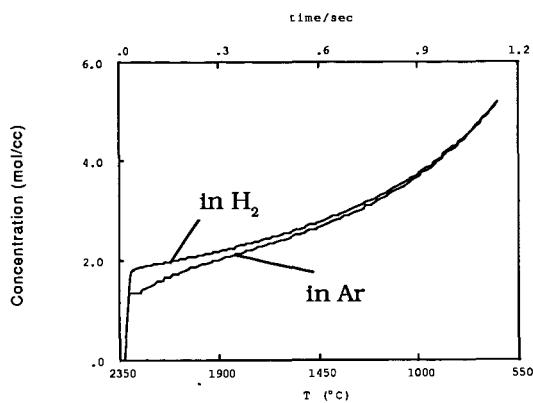


Fig. 3. Concentration of C_2H_2

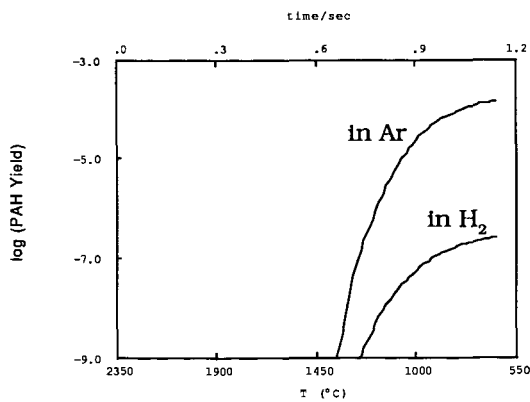


Fig. 4. Concentration of PAHs

SUPERSONIC BEAM STUDIES OF CARBON CONDENSATION

R. E. Smalley
Rice Quantum Institute and Department of Chemistry
Rice University
Houston, Texas 77251

INTRODUCTION

In the course of the current rage of fascination with how diamond growth may be nucleated and controlled, it is probably wise to consider in some detail the nature of the beast with which diamond growth must compete. The beast in this case is the growth of graphite either in its perfect crystalline form, or more typically in one of its less flat, often more tortuous morphologies. After all graphite is the most stable form of carbon under moderate pressure conditions, and diamond growth can dominate only as a result of some kinetic trick. Unfortunately, this will have to be a very powerful trick indeed, since it turns out that the kinetics of nucleation and growth of graphitic type objects are sensationally facile.

This short paper considers some of the newest evidence of just how formidable this graphitic beast is. Strangely, much of this new evidence has come from the rarified and esoteric environment of supersonic beams and laser spectroscopy. Advances in laser and supersonic molecular beam techniques over the past 5-10 years have produced a flood of new results and insights as to the nature of small clusters. Within the sub-field of strongly bound (non van der Waals) clusters, certainly one of the most active and intellectually exciting areas has been the study of carbon. Although many of these new experiments are still in the process of verification, extension, and further interpretation, a remarkable new picture is beginning to emerge as to some of the dominant processes of carbon condensation and the nature of the (largely graphitic) species involved.

Perhaps the most concise way to summarize this subject is simply to list some of the key features of the emerging new view of the small clusters of carbon.

- (1) Carbon nucleates to form small clusters far more readily than any other element in the periodic table (including such refractory metals as tungsten and tantalum or the semiconductors silicon, germanium, and gallium arsenide).
- (2) The smallest clusters (C_2 through C_{29}) are essentially one-dimensional: they are most stable in the form of linear chains or monocyclic rings (depending on the charge state and temperature).
- (3) Even-numbered clusters in the 32-100+ atom size range often take the form of entirely closed, hollow spheroidal

shells (the "fullerenes") made up of catacondensed networks of 5- and 6-membered rings. All such fullerenes contain exactly twelve 5-membered rings. Under certain conditions it is possible to trap any of a wide range of metal atoms inside the hollow cavity of these fullerene shells. This includes such metals as sodium, potassium, cesium, calcium, barium, strontium, lanthanum, and actinides such as uranium.

(4) Odd-numbered clusters in the 33-101+ atom size range often take the form of nearly-closed spheroidal shells (the "semifullerenes") also made up of 5- and 6-membered rings.

(5) The prototypical fullerene, C_{60} ("buckminsterfullerene"), prefers the shape of a truncated icosahedron. Because of its size and perfect symmetry, it is extremely stable (chemically, thermodynamically, photophysically). The strain of closure of the fullerenes tends to concentrate at the vertices of the pentagons. Only for C_{60} -- and only when it takes the perfectly icosahedral form -- is this strain uniformly distributed over all carbon centers. It is this symmetry-derived absence of concentrated strain that gives C_{60} its unique stability.

(6) The fullerenes appear to be made whenever carbon condenses, including sooting flames where they are the most abundant ions present above 300 amu.

(7) A spiraling shell is an interesting model for the active nucleus involved in carbon grain growth in space, and soot formation in combustion environments here on earth. It is sensible that this is the most likely graphitic growth form possible in condensing carbon vapors. In this view the fullerenes are best interpreted as side products (dead ends) in a growth process that ultimately produces macroscopic particles.

When compared to the view prevalent in the carbon literature only a few years ago, these 7 points (with the possible exception of the first two or three) are quite divergent -- perhaps even wildly divergent. Nonetheless, my colleagues and I have found the new experimental evidence compelling. To our knowledge this picture is the only one consistent with all experimental results, both new and old.

Within the scope of this short paper it is unreasonable to attempt a full review of the various experiments and lines of argument that have led to this new view. My colleagues and I have published extensively as this work has proceeded from the original experiments of Rohlffing, Cox, and Kaldor (1), and our subsequent realization that C_{60} is supremely special and probably spherical (2). Two fairly comprehensive and up-to-date reviews have recently appeared as articles in the journal Science (3,4). These serve well as both a summary of current evidence and beliefs (at

least as perceived the principal proponents), and as pointers to the relevant literature.

Instead, I will take this opportunity to dwell a bit on one central point of this story that is often misunderstood: the mechanism we have come to suspect is responsible for the facile formation of C_{60} and the other fullerenes. Like most mechanisms offered to explain chemical reactions, this one is highly conjectural. But it does offer a simple explanation for why hollow, spheroidal objects form with such facility. I bring it up in the context of this symposium on diamond growth since the conditions used in most of the current diamond film research are also those where such spheroidal, basically graphitic objects as the fullerenes would be expected to form as well. The thrust of the argument is that this fullerene formation mechanism may either be the "beast" himself, or at least a close associate.

A NEW GROWTH SENARIO FOR THE FULLERENES AND GRAPHITIC SOOT

To most observers the most unbelievable aspect of the buckminsterfullerene story was not that C_{60} may prefer the soccerball geometry. It was clear from the outset that this was a perfectly kosher bonding network for carbon which solved the problem of tying up all dangling bonds with beautiful symmetry and structural integrity. In fact it had been predicted to be stable, and its synthesis had been undertaken years before the supersonic cluster beam experiments were even conceived of at Rice University. What seemed truly incredible was the notion that such a huge, highly symmetric structure could pop full-formed out of something so simple and mindless as a carbon vapor. Particularly vexing was the question of why any molecule would naturally form with a such a huge vacuous cavity in the center. Whatever happened to Nature's supposed abhorrence of a vacuum?

Confronted with the clear fact that, regardless of intuition, C_{60} and the fullerenes are produced readily, and the compelling evidence that they did have the spheroidal cage structure, we searched for a rational growth mechanism. The growth senario we began to advocate was first sketched briefly in a few paragraphs of a short paper we submitted late in 1985 (5).

It seemed clear that the key topological event must involve some inherent tendency of a growing polycyclic aromatic net to curl. We are accustomed to think of aromatic carbon nets as rigid, flat plates. Certainly the vast majority of known polycyclic aromatic compounds are indeed flat (at least at absolute zero). More insidiously, the molecular model kits used to teach modern chemistry have engendered this notion of rigid, flat sp^2 carbon frameworks as though it were a central dogma of structural chemistry. This is a great model for ordinary closed shell aromatic molecules, but that is certainly not what one is dealing with when a pure carbon vapor condenses. Carbon networks growing at high temperature in the absence of hydrogen will have a

large number of dangling bonds, so it is by no means clear that perfect sp^2 hybridization should apply.

Instead we noted that simply by incorporating a pentagonal ring in the periphery of a growing hexagonal net, at least one good new carbon-carbon bond will always be formed from what was previously two dangling bonds. This pentagon causes the net to curl out of plane, the added strain of curvature being offset by the increased bonding.

Following along on this notion that curvature in a growing graphitic net would be a natural consequence of a local incentive to minimize dangling bonds, we supposed that if one pentagon was good, two would be better. But as a second-order consideration it should be noted that two adjacent pentagonal carbon rings is hardly ever encountered as a stable aromatic structure in ordinary polycyclic compounds (it is an antiaromatic cycle, and it concentrates strain). One should therefore expect a tendency for the growing graphitic sheet to incorporate pentagons offset from one another by intervening hexagons on the leading edge of the growth front.

That is basically all there is to the mechanism. There is a simple local tendency to minimize dangling bonds by incorporating pentagons on the growth front, and a weaker tendency to have these pentagons spaced by an intervening hexagon. Note that if followed perfectly, this simple growth rule forms a net which closes perfectly on itself -- it makes a C_{60} soccerball!

Under rapid growth conditions, with insufficient time and/or energy to anneal out mistakes and adhere slavishly to the lowest energy path, this mechanism would predict a wide range of fullerenes to form. Once formed, the absence of dangling bonds on these fullerenes effectively removes them from subsequent direct growth reactions. They can participate further in the condensation process only by adhering to each other, or by becoming sufficiently excited to break open at a site where strains have concentrated, thereby producing a point for further chemical attack and growth.

As we argued in the original paper (5), it seems likely that a rapidly growing graphitic net tying up dangling bonds by this simple rule will most typically fail to close. Instead it is easy to visualize one growth front curling over and burying the opposite edge inside to form the first turn of a 3-dimensional spiral. Once an edge is buried, there is no opportunity for the growth to stop, the spiral simply continuing to grow turn by turn until a macroscopic spherical carbon particle is produced. In fact such particles have been seen before with scanning electron microscopes (6). Such spherical carbon particles formed from pure condensing carbon we prefer to call "graphitic soot". Their ready formation is an unavoidable prediction of the fullerene growth mechanism.

CARBON GROWTH IN A HYDROGEN-RICH ENVIRONMENT

More relevant to the formation of ordinary soot in combustion environments -- and to the conditions where diamond film growth is sought in the experiments discussed in this symposium -- is the circumstance where there is an abundance of hydrogen. Since the fullerene growth mechanism we've been discussing is driven by the presence of dangling bonds, it's not immediately clear how it could apply when there is plenty of hydrogen around to tie up these dangling bonds. With enough hydrogen, one can make any graphitic sheet into a perfectly stable polycyclic aromatic hydrocarbon (PAH), and the most stable of these are always flat.

But at sufficiently high temperatures, hydrogen does not effectively tie up dangling bonds on carbon. Only another carbon atom can do that. Elementary chemical thermodynamics shows that most hydrocarbons are uphill with respect to graphite + H_2 even at room temperature. At the elevated temperatures encountered in flames this is even true for such species as methane and acetylene. The driving force for this is not so much the strength of the carbon-carbon bond in graphite. Instead it is primarily due to the high entropy of gaseous H_2 . Thermodynamically, that's why soot forms.

At elevated temperatures where a significant concentration of hydrogen atoms are present, the carbon-hydrogen bonds on the periphery of a PAH are not safe. Hydrogen abstraction reactions will proceed to generate a free H_2 molecule, leaving behind a bare, dangling bond on the now partially hydrogen-terminated graphitic network. Under sufficiently intense H atom attack, therefore, the fullerene growth mechanism discussed above should come into play. The only way such a molecule can tie up its dangling bonds is to use carbon. It will do this until it forms a stable fullerene, or if it misses the fullerene stage, it would be expected to spiral its way to a microscopic soot particle.

So it is conceivable that the fullerenes and spiral graphitic soot particles may be formed in sooting flames. Indeed Homann and his group have found C_{60} and the fullerenes to be very abundant as positive ions in flames (7). In my opinion this is a singularly vital experiment to be repeated and explored by other groups. Although currently the vast majority of the combustion community appears to disagree, to my reading the current evidence supports the notion that the fullerene growth mechanism is so facile in flames that it may be the mechanism responsible for the nucleation and early stages of soot growth in flames. Homann and his associates seem to have at least the beginnings of a method to give a critical test to this notion, but as yet there is no proof one way or the other.

FULLERENES UNDER DIAMOND GROWTH CONDITIONS

More relevantly to this symposium, it seems likely that fullerenes and the related graphitic spirals may be important species under diamond growth conditions. The conventional wisdom in the diamond film growth business is that graphitic (or "amorphous") carbon is constantly being nucleated as well as diamond on the growth surface, but that H atoms etch the non-diamond phases preferentially. The mechanism of this etching process is quite unclear, but there is little doubt that it is essential.

One obvious question is whether the etch process requires attack at an edge of a graphitic sheet. If it does, the presence of fullerenes will be a problem: they have no edges. In fact this suggests that an interesting line of research would be to study the susceptibility of large fullerenes to H atom attack. This turns out to be a vital issue in astrophysics as well. We have argued (2-4) that C_{60} in particular, and the fullerenes in general are likely to be made in vast quantities in the outer regions of carbon-rich red giant stars. Their abundance there, and their subsequent viability in space as they are driven from the star by photon pressure and the stellar wind will depend strongly on the ability to withstand H atom attack. It seems likely that there will be only a mild barrier to attaching a single H atom on one of the surface carbon atoms. But it may be a fairly weak bond, and do little to weaken the structural integrity of the fullerene cage. The lowest thermal dissociation process of such a H-fullerene would most likely be just a simple desorption of the H atom.

Beyond this question of getting rid of the fullerenes once formed, it is sobering consider the great efficiency of this fullerene condensation mechanism for carbon. Even in the absence of hydrogen, all the bare clusters of carbon starting from C_2 , extending through the last of the linear chains and monocyclic rings, to the curling polycyclic graphitic nets, to the fullerenes and the spiraling soot particles ... all of these species are abnormally strongly bound molecules. Unlike any other element, these species are formed almost instantly in a laser-produced vapor, and the final end point, graphite, is one of the most refractory species known.

The fullerene growth mechanism when it defaults to the formation of a spiral graphitic soot particle quickly generates an almost perfect graphite particle. It is mostly edgeless: if it forms optimally, its only edges are found on the last turn of the spiral, and on the innermost turn where the initial edge was buried. Since each layer of the spiral contains only 12 pentagons, the vast majority of the carbon atoms in such a structure are involved in hexagonal rings with only a tiny deviation from planarity. Remarkably, it turns out that the most perfect and symmetrical of these spiral soot particles (the one

that starts with an aborted C_{60} truncated icosahedron, and proceeds to a second layer of 240 atoms, a third of 540 atoms, etc.) naturally has each layer spaced from those above and below by 3.6 angstroms. This is almost exactly the normal interplanar spacing of bulk graphite. In other words, these spiral graphitic particles are macromolecular (but still microscopic) forms of graphite. They may be expected to form with extraordinary speed, and be highly stable. For diamond film growers this is a beast that, once conjured up, may be rather difficult to slay.

ACKNOWLEDGEMENT

The author wishes to acknowledge Robert Curl, Harry Kroto, and Jim Heath for extensive, expansive discussions; and David Nelson who stimulated these thoughts toward diamond. Supersonic carbon cluster research at Rice University was funded by the National Science Foundation and the Robert A. Welch Foundation. Our bare metal cluster research is funded by the Department of Energy, Division of Chemical Sciences, while that on semiconductor clusters was funded by the Office of Naval Research and (for gallium arsenide) the US Army Research Office.

REFERENCES

- (1) Rohlfing, E. A., Cox, D. A., and Kaldor, A. J. Chem. Phys., 1984, 81, 3322.
- (2) Kroto, H. W., Heath, J. R., O'Brien, S. C., Curl, R. F., and Smalley, R. E., Nature, 1985, 318, 162.
- (3) Curl, R. F., and Smalley, R. E., Science, 1988, 242, 1017.
- (4) Kroto, H. W., Science, 1988, 242, 1139.
- (5) Zhang, Q. L., O'Brien, S. C., Heath, J. R., Liu, Y., Curl, R. F., Kroto, H. W., and Smalley, R. E., J. Phys. Chem., 1986, 90, 525.
- (6) Iijima, S., J. Phys. Chem., 1987, 91, 3466.
- (7) Gerhardt, Ph., Loffler, S., and Homann, K. H., Chem. Phys. Lett., 1987, 137, 306.

THE ROLE OF IONS IN SOOT AND DIAMOND FORMATION

H. F. Calcote
AeroChem Research Laboratories, Inc.
P.O. Box 12, Princeton, NJ 08542

INTRODUCTION

Soot and diamonds are different forms of carbon. It is thus natural to examine mechanisms which have been proposed for the formation of soot with respect to the mechanism of diamond film deposition. Frenklach and Spear have done this with respect to the free radical mechanism of soot formation (1). Diamond deposition is frequently a plasma process and ions have been proposed in several mechanisms to explain the process. There is considerable evidence (2) of an ionic mechanism of soot formation. The demonstration that diamonds can be deposited from combustion flames (3, 4) also makes it timely to consider soot forming processes in flames as they might relate to diamond deposition. Thus we briefly review the ionic mechanism of soot formation and the evidence for an ionic role in diamond deposition; we then make a few observations relevant to the role of ions in the mechanism of diamond deposition.

IONS IN SOOT FORMATION

The ionic mechanism of soot formation, Figure 1, postulates that chemiions, HCO^+ and C_3H_3^+ , which are present in excess of equilibrium in hydrocarbon flames, rapidly grow by ion-molecule reactions in which several neutral species continue to add to an increasingly larger ion. As an ion becomes larger, it is neutralized by the electrons produced in the chemiionization reactions. This process gives both charged and neutral incipient soot particles which continue to grow by the addition of acetylene and other small neutral species. There are two important considerations in the ionic mechanism: (1) the large rate coefficients for ion-molecule reactions, and (2) the rapid isomerization of ions to produce a cyclic structure. Formation of the first ring is the main problem with the neutral mechanism and has absorbed much of the research attention relevant to the neutral mechanism.

The soot concentration, in many flames, is in excess of equilibrium so must be driven by a species whose concentration exceeds equilibrium. Chemiionization is a nonequilibrium process producing ionic concentrations orders of magnitude in excess of equilibrium.

In Figure 1, the direct path to C_3H_3^+ appears unimportant in flames (5) but may be important in pyrolysis systems producing soot, where ions are also observed (6). Therefore C_3H_3^+ is probably generated by a series of ion-molecule reactions from HCO^+ . The ion C_3H_3^+ grows by adding small neutral species in a series of ion-molecule reactions, in which any one of the growth species, see, e.g., Figure 1, may add to a given ion to produce a larger ion. At each stage the ion may also be neutralized by reaction with an electron produced in the initial chemiionization step. The product of this reaction, usually a dissociative recombination, is identified in Figure 1 as "neutral reactant" (e.g., a polycyclic aromatic hydrocarbon) and this neutral species may continue to grow by a neutral free radical mechanism, also leading to an incipient soot particle.

All of the ions proposed in the ionic mechanism have been observed in flames up to mass 557 amu; the concentration of ions has been demonstrated experimentally to be sufficient to account for the concentration of soot measured; and the rates of ion formation in both premixed (7) and diffusion (2) flames are about the same order of magnitude as the rate of soot formation.

IONS IN DIAMOND FORMATION

Diamond films have been deposited by many different techniques including electrical discharge systems, e.g., microwave, rf, and dc glows; dc and rf arcs; and arc jets. They have also been made with ion beams, combustion flames, and hot filaments. The electrical discharge systems are based upon electrically driven plasmas. From the above discussion, it is clear that the combustion system is also a plasma. This leaves only the hot filament technique as not obviously involving a plasma.

It has been demonstrated, however, that in the hot filament technique, the application of an electric field to the substrate can influence the rate of diamond film deposition. Yarbrough (8), e.g., found that a positive voltage on the substrate increased the rate of diamond deposition and a negative voltage prevented deposition. This indicates the importance of charged species in the deposition process and puts this system as well in the plasma category. The source of the ionization is most likely electron emission from the hot filaments which were tantalum tubes heated to 2370 to 2470 K (9). Thus all diamond preparation systems have a unifying feature--the presence of ions.

In a magneto-microwave plasma, Susuki et al. (10) also observed the rate of film deposition to be accelerated by application of a positive electric field to the substrate. In these two systems, observations indicate either diamond deposition enhancement by negative ions or electrons, or an inhibiting effect by positive ions.

On the other hand, others have found that accelerating positive ions toward the substrate surface enhances the rate of diamond deposition (11), or more generally the application of a negative bias to the substrate increases the rate of film deposition or alters the properties of diamond (12) or diamond-like (13) films.

MECHANISTIC IMPLICATIONS

Since a plasma generated by an electric field is a common component of many diamond film deposition processes, we examine the process of creation of active species in an electrical discharge device. Most deposition processes use a mixture of hydrogen containing a few percent methane, so we examine the chemistry expected in this system. In Figure 2 the electron energy distribution for three different electron temperatures is presented along with the collision cross section for the initial reactions by which electric power is coupled to the gas. There are several points to be made from this figure. First, the electron temperature must be very high compared to deposition temperatures, typically 800-1300 K, for a significant percentage of the electrons to dissociate or ionize the reactants. Even in a low temperature discharge, measured by the gas temperature, the electron energy must be high enough to produce ions to maintain the discharge. For hydrogen and methane, dissociation occurs at electron energies, 3 to 6 eV below where ionization sets in; higher cross sections are reached at the energies at which ionization sets in. Yet, to maintain the discharge, ionization must occur, so that some of the electrons have energies in the neighborhood of 14 to 18 eV.

Thus the initial reactive species concentrations are present at equivalent temperatures far above the gas temperature and certainly far above the substrate temperature. The initial system is far from equilibrium and any modeling of the process must start with this condition. The nonequilibrium condition is, of course, consistent with the fact that diamond is thermodynamically metastable with respect to graphite. The chemistry occurring between the super-equilibrium formation of active species and their striking the substrate surface is of interest. Thus models must start with the formation of active species and these may be different for the many techniques which have been used to produce diamond and diamond-like films.

The question of whether ions or free radicals play the dominant role in electrical discharge chemistry has not been resolved and must depend upon the specific system (see e.g., Avni and coworkers (17) or Marcus and Platzner (18)). Ion-molecule reaction rate coefficients are orders of magnitude greater than free radical rate coefficients but the ions are generated in smaller initial concentrations. Further, as ions recombine with electrons, also a very rapid process, they dissociate to produce hydrogen atoms or free radicals, e.g.,



Thus the nonequilibrium formation of ions plays a role in the production of super-equilibrium concentrations of hydrogen atoms and free radicals. H atoms are considered important in suppressing graphite buildup in competition with the deposition of diamonds (19), as well as in abstracting hydrogen atoms from the growing surface.

The observations that electric fields affect the rate of diamond deposition and the fact that plasmas contain ions, have led to proposals that ions are important in diamond deposition (11, 13, 20). All of these proposals incorporate positive ions, e.g., CH_3^+ in the mechanism. Tsuda et al. (20) describe a mechanism for diamond growth in which the diamond surface first becomes covered by methyl groups and then a methyl cation strikes the surface, simultaneously binding three methyl carbons to form the diamond structure. This concerted process does not allow the surface to graphitize. A very detailed mechanism is developed for which an activation energy of 27.4 kcal/mol is deduced. This is less than measured activation energies for diamond deposition which lie between 55 kcal/mol (19, 21) and 80 kcal/mol (19).

In the Frenklach-Spear mechanism (1) a hydrogen atom abstracts a hydrogen atom from a surface site where an acetylene molecule then adds. They develop a kinetic scheme from which an energy barrier of only 17.4 kcal/mol is obtained, even lower than for the Tsuda et al. mechanism and even further below the measured activation energy!

The implication of the importance of ions, because of the effect of electric fields, on the deposition of diamonds, coupled with the probably small concentration of ions relative to free radicals and other neutral species, suggests a mechanism in which an ion plays the role of a catalyst or the seed in a nucleation step, neutrals providing much of the ultimate mass.

The effectiveness of both positive and negative voltages clouds the picture. The source of positive ions is clear, but if negative ions, rather than electrons, are important, their source is not clear. Electron attachment may form a route for the formation of negative ions in hot wire or electrical discharge systems used to prepare diamond films. However, a calculation of the equilibrium constants from the free energies of formation as a function of temperature, shows that among the simple neutral species expected in the H_2/CH_4 system, the attachment of an electron to a hydrogen atom or CH radical is a candidate; equilibrium favors H^- below about 1800 K and CH^- below about 2200 K. The hydrogen reaction would require a third body. In the case of the hot filament, the negative ions could be formed on the filament. Catalytic decomposition or thermal decomposition could account for other species, including possibly, ions of both signs.

Negative ions have been observed (22, 23) in sooting flames but they have not been identified mass spectrometrically; they are assumed to be large molecular ions produced by electron attachment. In somewhat leaner, nonsooting flames, negative ions have also been identified, Figure 3, but their mechanism of formation is vague; they do not seem to be formed by simple attachment (24). They are present at about 1% of the positive ion concentration at an equivalence ratio of 1, stoichiometric flames, and their maximum concentration occurs at a higher equivalence ratio, fuel rich, than for positive ions. Their concentrations decrease with increasing total pressure. To my knowledge no measurements of the effect of voltage on diamond deposition in combustion systems have been made. Interestingly, diamonds are deposited from the flame in the region where soot is formed and where ions are present (25).

The growth species which adds to the ionic nuclei may be a stable molecule e.g., acetylene as suggested by Frenklach and Spear (1) or the methyl radical which has frequently been suggested (20). Angus (21) measured the rate of deposition of diamond in a hot filament environment to be first order in the methane pressure and one-half order with respect to ethylene pressure, from which he deduced that the growth mechanism must involve the addition of a species containing only one carbon atom. Similarly, Sato, Kamo, and Setaka (26) examined the effect of hydrocarbons, including alkanes, alkenes and acetylene on growth and Raman spectra of diamond films prepared in a microwave system and concluded that growth features and morphology are dependent approximately on the number of carbon atoms in the molecule. On the other hand, Fedoseev and associates (19) observed that the highest activation energy and the lowest rates were associated with growth from methane, and the lowest activation energy and the highest rates were associated with acetylene and that other hydrocarbons fell between these. This is reminiscent of the effect of molecular structure on both ion formation and soot formation in flames (2). Is there a connection?

CONCLUSIONS

The plasma condition seems to be a prerequisite for diamond film deposition, even by the hot filament technique and from a combustion flame. The ions in the plasma are at a concentration

considerably in excess of their equilibrium concentration at the substrate temperature, as are free radical and hydrogen atoms. Thus any model of the process must start with these conditions in the plasma. Both positive and negative ions (or electrons) seem to be involved. The source of positive ions is fairly clear, but the source and nature of negative ions are not. Because of the low concentration of ions compared to other species it is most likely that their role in diamond coating technology is analogous to that in flames, i.e., they act as nucleation agents, not as growth species.

ACKNOWLEDGEMENTS

Drs. David Keil and Robert Gill's helpful discussions are gratefully acknowledged, as is Dr. Gill's calculation of the heats of formation of the negative hydrocarbon ions as a function of temperature.

REFERENCES

- (1) Frenklach, M. and Spear, K.E. *J. Mater. Res.*, 1988, 3, 133.
- (2) Calcote, H.F., Olson, D.B., and Keil, D.G. *Energy & Fuels*, 1988, 2, 494.
- (3) Carrington, W.A., Hanssen, L.M., Snail, K.A. Oakes, D. and Butler, J.E., "Diamond Growth in $O_2+C_2H_4$ and $O_2+C_2H_2$ Flames" submitted to *Metallurgical Transactions*, 1988.
- (4) Hirose, Y. and Konda, N., Japan Applied Physics, 1988 Spring Meeting, p. 434.
- (5) Eraslan, A.N. and Brown, R.C., *Combust. and Flame*, 1988, 74, 19.
- (6) Kern, R.D., Singh, H.J., and Xie, K. "A Systematic Search for the Presence of Chemi-ions in Pyrolytic and Oxidation Systems" 22nd Symp. (Int.) on Combustion, Seattle, Washington, August 14-19, 1988, Poster 100.
- (7) Keil, D.G. and Calcote, H.F. unpublished work.
- (8) Yarbrough, W. A., The Pennsylvania State University, personal communication, 10 November 1987.
- (9) Yarbrough, W.A. and Roy, R., "Nanocomposite Diamond Films by Hot Filament Assisted CVD," MRS Extended Abstracts, Diamond and Diamond-Like Materials Synthesis, G.H. Johnson, A. R. Badzian, and M. W. Geis, Eds., April 5-9, 1988, 33.
- (10) Susuki, J.I., Kawarada, H., Mar, K.S. Yokota, Y., and Hiraki, A. "Large Area CVD of High Quality Diamond Films Using High-Density Magneto-Microwave Plasma at Low Pressure," Paper No. T3, Diamond Technology Initiative Symposium, Arlington, VA 12-14 July 1988.
- (11) Namba, Y., Japan Applied Physics, 1987 Fall Meeting, Abstract 17P-A-1.
- (12) Hirata, T. and Nage, M., MRS Extended Abstracts Diamond and Diamond-Like Materials Synthesis, G.H. Johnson, A. R. Badzian, and M. W. Geis, Eds., April 5-9, 1988, 49.
- (13) Koidl, P. and Wild, CH., MRS Extended Abstracts Diamond and Diamond-Like Materials Synthesis, G.H. Johnson, A. R. Badzian, and M. W. Geis, Eds., April 5-9, 1988, 41.
- (14) Rapp, D. and Englander-Golden, P. *Journal of Chemical Physics*, 1965, 43, 1464.
- (15) Winters, H.F. *Journal of Chemical Physics*, 1975, 63, 3462.
- (16) Corrigan, S.J.B. *Journal of Chemical Physics*, 1965, 43, 4381.
- (17) Avni, R., Carmi, U., Inspector, A., and Rosenthal, I. *Journal of Vacuum Science and Technology*, 1985, A3, 1813.

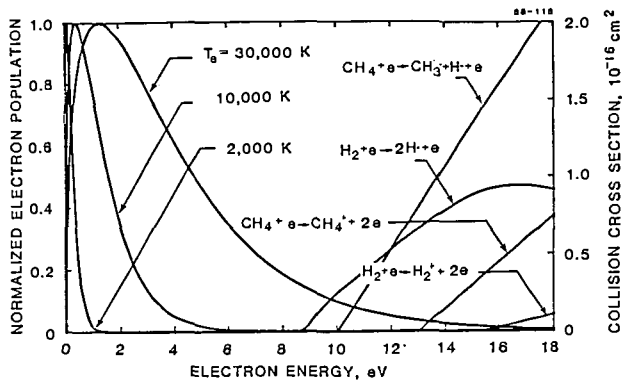


Figure 2. Electron Collision Dissociation of Methane and Hydrogen
 Ionization of Methane from Ref. 14.
 Dissociation of Methane from Ref. 15.
 Dissociation and Ionization of Hydrogen from Ref. 16.

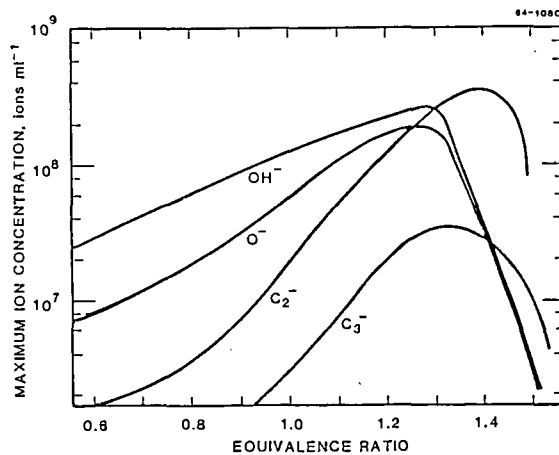


Figure 3. C_2H_2/O_2 Flame at 0.27 kPa.
 Total Flow = 70 cm³/s (STP).

GAS PHASE KINETICS DURING DIAMOND GROWTH: CH₄ AS GROWTH SPECIES

Stephen J. Harris
Physical Chemistry Department
General Motors Research Labs
Warren, MI 48090

Introduction

There has been considerable interest in the growth of diamond thin films in recent years^{1,2}. This interest derives from the superlative properties of diamonds: they are very hard, have a high thermal conductivity, are chemically inert, and have an extremely wide optical transmission window. In addition, single crystal diamonds have the potential for being uniquely good semiconductors².

Unfortunately, at present we have little understanding of the chemical processes which are involved in and which control diamond nucleation and growth. This is because there have been no experiments which have simultaneously characterized both the chemical environment and the kinetics of diamond growth. Recently C₂H₂ (acetylene)^{3,4}, C₂H₄ (ethylene)³, CH₃ (methyl radical)³, and H (atomic hydrogen)³ have been detected during filament-assisted diamond growth experiments. Harris et al.⁴ used a simple zero-dimensional chemical kinetics model to show that only CH₄ (methane), C₂H₄, C₂H₂, and/or CH₃ could be contributing significantly to surface growth in those experiments. This result is consistent with semi-empirical quantum mechanical studies of the diamond growth mechanism which suggest that the growth species is either C₂H₂⁵ or CH₃⁶.

Earlier detailed measurements of the kinetics of diamond growth on diamond seed crystals from CH₄-H₂ mixtures were made by Chauhan, Angus, and Gardner⁷. Although the chemical species present were not determined in their work, we recognized that the gas phase chemistry could be approximately modeled based on the information that was provided. In this work we analyze the data of Chauhan et al.⁷ to determine which species accounted for the diamond growth that was observed.

Analysis

The experiments of Chauhan et al.⁷ were carried out on a microbalance which allowed the rate of diamond growth to be measured. For the particular experiment that we modeled, labeled 44-C, a 0.5 torr mixture of 70% CH₄ and 30% H₂ passed through a cylindrical 2.54 cm diameter flow tube into the top of a spherical 10.16 cm diameter pyrex reaction chamber, at the center of which was suspended a crucible holding 98.934 mg of diamond seed crystals. The gases were pumped away at the bottom of the reaction chamber through a 3.81 cm diameter flow tube. The seed crystals, which had a BET surface area of 7 m²/g, were heated to 1438 K by radiation from a lamp; there were no other heaters in the system. The wall temperature of the reaction chamber was maintained below 500 K, eliminating heterogeneous pyrolysis chemistry there. The gas velocity was not specified, but Chauhan et al.⁷ stated that the gases flowed at a rate "such that the methane available was more than 50 times that required to obtain the observed deposition rates." This implies an input flow velocity of at least 94 cm/s, readily achieved in flow tubes of this size. Chauhan et al.⁷

determined that all of the initial weight gain as monitored by the microbalance was due to diamond, although as time progressed more and more of the weight gain came from non-diamond (pyrolytic) carbon. In this work we model only the initial growth period, before any formation of pyrolytic carbon.

The measurements of Chauhan et al.⁷ showed an initial fractional growth rate of

$$\frac{1}{m} \frac{dm}{dt} = 1.31 \times 10^{-3} \text{ min}^{-1}, \quad (1)$$

where m is the mass of the diamond crystals. This rate corresponds to a specific surface growth rate of 3.1×10^{-10} g/cm²·s. For a growth species depositing n_c carbon atoms with each reaction, Eqn. (1) implies that $1.6 \times 10^{13}/n_c$ molecules reacted/cm²·s. This reaction rate is equal to the collision rate of growth species with the diamond surface (calculated from the kinetic theory of gases⁸) times the reaction probability R that a given collision leads to reaction,

$$\frac{1.6 \times 10^{13}}{n_c} = 3.52 \times 10^{22} \frac{P}{\sqrt{MT}} R, \quad (2)$$

where P is the growth species pressure in torr, M is the molecular weight of the growth species, and T is the temperature in degrees Kelvin. For $M = 15n_c$ and $T = 1438$ K, the growth species mole fraction is $X = 1.3 \times 10^{-7}/R\sqrt{n_c}$. Since $R \leq 1$ the mole fraction for the growth species must be at least $X_{\min} = 1 \times 10^{-7}$ (0.1 parts per million) for reasonable (i.e., small) values of n_c . This is our first constraint on the growth species.

Diamond growth acts as a sink for growth species, so in order to maintain a *steady state* concentration greater than X_{\min} the growth species must not be depleted faster than they are created and transported to the diamond seed crystals for reaction. From Eqn. (1), the diamond growth rate was 2.2×10^{-6} g/s, all of which mass must ultimately have come from CH_4 . This implies that at least 8.1×10^{16} CH_4 molecules reacted per second, and that at least $8.1 \times 10^{16}/n_c$ growth species were formed per second (unless CH_4 was itself the growth species). This is our second constraint on the growth species.

We have modeled the gas phase pyrolysis chemistry in this system in order to determine which hydrocarbons satisfied these two constraints in the system of Chauhan et al.⁷ Several approximations and assumptions were used; these are discussed in a separate section below.

The experiment is modeled as follows. We assume 1-dimensional flow so that the gas temperature and species concentrations depend only on the distance Z along the tube or reaction chamber. The gas is assumed to enter the 2.54 cm diameter flow tube at $Z = 0$, $T = 300$ K, and $v_0 = 94$ cm/s. The gas flows into the reaction chamber at $Z = 35.1$ cm and $T = 500$. Beyond that point the gas temperature is assumed to rise linearly with Z until it reaches a maximum of 1438 K at the crucible, taken to be at $Z = 40$. The temperature then falls slowly (heat loss to the relatively distant reaction chamber walls assumed small) to 1250 K as it exits the reaction chamber at $Z = 44.7$. For $Z > 44.7$, where the gas is again in a flow tube, the temperature drops to 500 K by $Z = 85$ cm. The gas velocity in the system is calculated assuming that the flux is given by $\rho v A = \text{constant}$, where ρ is the gas density and A is the cross sectional area of the tube or reaction chamber. We estimate that $v = 28$ cm/s at the crucible and that the gas has a residence time in the reaction chamber of 250 ms. The gas phase chemistry is modeled using the Sandia burner code⁹ together with

the reaction mechanism shown in Table I. A similar mechanism was successful in predicting the species concentration profiles in a number of premixed flat flames^{10,11}. Although the mechanism considers species as large as C_4H_6 , only the C_1 and C_2 part of the mechanism is shown since the concentrations of larger species are always extremely small and since the C_3 and C_4 chemistry is less well known. The pressure-dependent reactions shown in the Table are in the low pressure limit. Rate constants $k = AT^n e^{-E_a/RT}$ are given for the forward direction; rate constants for the reverse direction are calculated using thermodynamic data from the Chemkin data base¹², supplemented where necessary by other standard sources¹³.

Results

The predictions of the model are shown in Figure 1, which displays steady state profiles of all species that reach mole fractions of at least 10^{-14} . The reaction chamber is located between $Z = 35.1$ and 44.7 cm, and the crucible is located at $Z = 40$.

Chemical reaction is initiated in this system by the reverse of Reaction 2 of Table I (denoted A_{-2}) which produces H and CH_3 and which occurs only at the highest temperature positions near $Z = 40$. The H is rapidly consumed by A_3 , forming additional CH_3 . Within the reaction chamber the CH_3 mole fraction (and the mole fractions of many other species) is nearly independent of Z because the gas velocity there is low, and mixing by diffusion is rapid. As the CH_3 formed by A_{-2} and A_3 diffuses upstream toward the flow tube, it is consumed by A_{-3} , creating H atoms. CH_3 decay for $Z < 35.1$ is due mainly to A_{-14} , which is nearly irreversible at the low temperatures in the flow tube. C_2H_6 , formed mainly between $Z = 33$ and $Z = 35$ by A_{-14} , is for the most part carried downstream into the reaction chamber. However, some C_2H_6 diffuses upstream against a high gas velocity, giving the falloff in concentration for $Z < 34$. C_2H_5 (ethyl radical) is formed in the reaction chamber by both A_{12} and A_{13} , but near $Z = 40$ it decomposes rapidly via A_{15} to make C_2H_4 , accounting for the drop in the C_2H_5 mole fraction there. A_{17} produces small amounts of C_2H_2 at $Z = 40$. Some C_2H_4 and C_2H_2 formed there diffuse upstream into the flow tube.

Because of the low pressure (0.5 torr) and short residence time (250 ms) in the reaction chamber, the chemical reactions are far too slow for the CH_4/H_2 mixture to attain equilibrium. For example, at equilibrium the mole fraction of C_2H_2 at the crucible would be 0.19, thirteen orders of magnitude higher than shown in Figure 1. The equilibrium mole fractions of some other relevant species are $X_{CH_4}^{eq} = 3.2 \times 10^{-4}$, $X_H^{eq} = 2.8 \times 10^{-4}$, $X_{C_2H_4}^{eq} = 4.8 \times 10^{-5}$, $X_{C_2H_6}^{eq} = 3.6 \times 10^{-6}$, and $X_{CH_3}^{eq} = 2.7 \times 10^{-6}$. Comparing these values to those shown in Figure 1, it is clear that the assumption of equilibrium is totally unjustified in this system. We showed previously⁴ that the assumption of equilibrium is equally untenable during filament-assisted diamond growth. Instead, the compositions in these systems are kinetically controlled.

Discussion

The first conclusion we draw from Figure 1 is that aside from CH_4 ($X = 0.7$), only C_2H_6 and CH_3 have mole fractions above $X_{min} = 1 \times 10^{-7}$. Using Eqn. (2), we can calculate the reaction probability R required if we assume that one of these species is responsible for the observed diamond growth. The result is $R_{CH_4} \sim 10^{-7}$, while $R_{C_2H_6}$ and $R_{CH_3} \sim 10^{-1}$. To put these numbers into perspective, the reaction probability for CH_4 decomposing on pyrolytic carbon¹⁴ is 1.5×10^{-8} at 1438 K, with a roughly similar reaction probability for

C_2H_6 ¹⁵. Based on these data, the value required here for R_{CH_4} appears quite reasonable while that for $R_{C_2H_6}$ does not. On the other hand, a high value for R_{CH_3} is plausible, as CH_3 is a radical. $X_{C_2H_4}$ and especially $X_{C_2H_2}$ are so small that these species can be excluded from further consideration.

Although X_{CH_3} and $X_{C_2H_6}$ both exceed X_{min} , we must also consider our second constraint and estimate the rate that CH_3 and C_2H_6 could have been generated from CH_4 decomposition. For purposes of this analysis we will make two extreme assumptions: (1) Every molecule of CH_4 which reacted at all was converted permanently into CH_3 or C_2H_6 . That is, we ignore all reactions such as A_{-3} which destroyed either species. (2) No matter where in the system these species were formed, they were transported to the crucible for addition to the diamond seed crystals. With these two assumptions we can calculate an upper limit to the rate of diamond growth from CH_3 and C_2H_6 .

Our analysis shows that at steady state approximately 95% of the CH_4 that reacted did so via A_3 , with nearly all the rest reacting via A_{-2} . Thus, we can calculate the total number of CH_4 molecules reacting/s by evaluating for each Z the rates of these 2 reactions, shown in Figure 2, multiplying them by the volume element $dV = AdZ$, and then integrating with respect to Z . The result is that the calculated steady state reaction rate integrated over the entire apparatus is 1.8×10^{14} CH_4 molecules/s. Since this rate is nearly 500 times lower than that required by our second constraint, we conclude that neither CH_3 nor C_2H_6 (nor any other species) was produced in this system at a rate fast enough to contribute significantly to diamond growth. We infer that diamond growth occurred in this system by direct decomposition of CH_4 on the diamond surface.

It is interesting to compare growth of diamond from CH_4 with growth of pyrolytic carbon from C_2H_2 . The kinetics of the latter reaction can be described using a single Arrhenius expression between 600 and 1700 K with an activation energy of only 25 kcal/mole^{16,17}. Since it is unlikely that a reaction involving radicals made from C_2H_2 would have such a low activation energy at 600 K, we expect that the acetylene reaction forming pyrolytic carbon is also a direct molecular decomposition on the carbon surface. It is, however, substantially faster than the decomposition of CH_4 to make pyrolytic carbon or diamond.

As pointed out above, the value we obtained here for R_{CH_4} is similar to that for CH_4 decomposition on pyrolytic carbon^{14,16}. Furthermore, the 55 kcal/mole activation energy measured by Chauhan et al.⁷ (or the 58 kcal/mole activation energy measured by Tesner et al.¹⁸ for the same reaction) is similar to the 65 kcal/mole for addition of CH_4 to pyrolytic carbon¹⁷. Finally, we note that H_2 acts as an inhibitor to growth of both diamond⁷ and pyrolytic carbon¹⁴ in CH_4 systems. It is tempting to imagine that diamond and pyrolytic carbon growth are similar processes. If so, we would speculate that diamond—like pyrolytic carbon—can grow from a direct reaction of a variety of hydrocarbons¹⁶, although the reaction probabilities for different species could vary considerably. Continuing with this line of speculation, the propensity of different growth species to form pyrolytic carbon (rather than diamond) could be different. For example, a molecule such as C_2H_2 , with its multiple bonds, could be more likely to form pyrolytic carbon than CH_4 , which is already sp^3 bonded. (However, even CH_4 does produce pyrolytic carbon.) In that case, since the C_2H_2 concentration increases approximately as the square of the CH_4 concentration when CH_4 is the starting material, we would expect a deterioration in the quality of the diamond films grown with increasing CH_4 concentration. Such a deterioration is in fact observed².

Although one of the main conclusions of this work is that the diamond growth results of Chauhan et al.⁷ cannot be accounted for by C_2H_2 or CH_3 , we emphasize that our results do not contradict the calculations of Frenklach and Spear⁵ or Tsuda et al.⁶, who claimed that C_2H_2 or CH_3 is the principal growth species in filament- or plasma-assisted diamond film growth. Our results show, instead, that diamond films *can and do* grow from CH_4 , and that neither C_2H_2 nor CH_3 is required. However, given the roughly similar concentrations of CH_4 , CH_3 , C_2H_4 , and C_2H_2 under filament-assisted diamond growth conditions^{3,4}, C_2H_4 , C_2H_2 and/or CH_3 could well contribute more than CH_4 to diamond growth there.

Because some of the experimental parameters used in this modeling effort were not measured, we had to make a number of approximations and assumptions. In this section we consider how they affect our conclusions.

The most important approximation is that the temperature and species mole fraction fields were 1-dimensional. In fact, the wall temperatures were stated to be below 473 K, even at the location we have called $Z = 40$, where we have assumed a temperature of 1438 K. And we have not accounted for radical destruction which can take place on the walls. Thus, for both temperature and chemical reasons the walls are sinks for radicals. Because of the importance of diffusion in this system, processes which occur at the walls can be expected to have an impact at the crucible, 5 cm away. In our model we can simulate the presence of such a sink 5 cm from the crucible by changing the assumed temperature profile so that it drops to 500 K (instead of 1250 K) by $Z = 45$. This results in reductions by factors of 2-3 in X_{CH_3} and X_H and factors of 4-6 in $X_{C_2H_2}$ and $X_{C_2H_4}$. By no means does this simple exercise accurately take into account the effect of the walls. What it does show, however, is that the presence of the cool walls lowers the mole fractions of the pyrolysis products (species other than CH_4 and H_2). We conclude that the mole fractions shown in Figure 1 are upper limits to their true values, reinforcing our conclusion that no species besides CH_4 could have contributed significantly to diamond growth.

Beyond considering the walls as radical sinks, we have not attempted to model any possible heterogeneous chemistry taking place in this system. We do not expect that extraneous heterogeneous chemistry affected the diamond growth kinetics for three reasons. (1) The rate for pyrolytic carbon growth measured by Chauhan et al.⁷ is within a factor of 2 of the rate of pyrolytic carbon growth calculated from the formula of Fedoseev et al.¹⁴ for the same CH_4 and H_2 pressures but in the absence of any diamond. Since this difference is smaller than the experimental uncertainty, we conclude that the presence of diamond has no effect on the growth rate of pyrolytic carbon. Similarly, the analysis of Chauhan et al.⁷ shows that the presence of pyrolytic carbon does not affect the growth rate of diamond (except to the extent that it reduces the available diamond surface area). These results make plausible the assumption that extraneous heterogeneous chemistry on the diamond also did not affect the kinetics of diamond growth. (2) The kinetics of diamond growth was the same in flow tubes with hot (~ 1200 K)^{18,19} and cool (< 500 K)⁷ walls. We conclude that heterogeneous chemistry on walls of the system did not affect the kinetics of diamond growth. (3) The kinetics of diamond growth was unaffected when platinum, graphite, or quartz were used as crucibles^{7,19}. That even a highly active catalytic material such as platinum did not affect the kinetics of diamond growth is perhaps not surprising if the growth species was CH_4 .

References

1. R.C. DeVries, *Ann. Rev. Mater. Sci.* **17**, 161 (1987).
2. J.C. Angus and C.C. Hayman, *Science* **241**, 913 (1988).
3. (a) F.G. Celli, P.E. Pehrsson, H.-t. Wang, and J.E. Butler, *Appl. Phys. Lett.* **52**, 2043 (1988). (b) F.G. Celli, P.E. Pehrsson, H.-t. Wang, H.H. Nelson, and J.E. Butler, Second Diamond Technology Initiative Symposium, paper W-2, July 13, 1988.
4. S.J. Harris, A.M. Weiner, and T.A. Perry, *Appl. Phys. Lett.*, **53**, 1605 (1988).
5. (a) M. Frenklach and K.E. Spear, *J. Mater. Res.* **3**, 133 (1988). (b) M. Frenklach and K.E. Spear, Second Diamond Technology Initiative Symposium, paper W-8, July 13, 1988.
6. (a) M. Tsuda, M. Nakajima, and S. Oikawa, *J. Am. Chem. Soc.* **108**, 5780 (1986). (b) M. Tsuda, M. Nakajima, and S. Oikawa, *Japanese J. Appl. Phys.* **26**, L527 (1987).
7. a. S.P. Chauhan, J.C. Angus, and N.C. Gardner, *J. Appl. Phys.* **47**, 4746 (1976).
b. S. P. Chauhan, "Diamond Growth from Vapor at Low Pressurs," Thesis, Chemical Engineering Division, Case Institute of Technology, 1972.
8. G.A. Somorjai, "Principles of Surface Chemistry," Prentice-Hall, New Jersey.
9. (a) M.D. Smooke, *J. Comp. Phys.* **48**, 72 (1982). (b) R.J. Kee, J.F. Grcar, M.D. Smooke, and J.A. Miller, Sandia Report SAND85-8240, 1985.
10. S.J. Harris, A.M. Weiner, R.J. Blint, and J.E.M. Goldsmith, *Twenty-first Symposium (International) on Combustion*, The Combustion Institute, 1033 (1986).
11. S.J. Harris, A.M. Weiner, and R.J. Blint, *Combust. Flame* **72**, 91 (1988).
12. R.J. Kee, F.M. Rupley, and J.A. Miller, Sandia Report SAND87-8215, 1987.
13. (a) D.R. Stull, E.F. Westrum, and G.C. Sinke, *Chemical Thermodynamics of Organic Compounds*, Wiley, New York, 1969; (b) A. Burcat in *Combustion Chemistry* (W.C. Gardiner, Ed.), Springer-Verlag, New York, 1984, p. 455.
14. D.V. Fedoseev, S.P. Vnukov, and V.P. Varnin *Dokl. Akad. Nauk* **218**, 399 (1974).
15. D.V. Denisevich and P.A. Tesner, *Dokl. Akad. Nauk* **212**, 660 (1973).
16. S.J. Harris and A.M. Weiner, *Ann. Rev. Phys. Chem.* **36**, 31 (1985).
17. E.F. Aref'eva, I.S. Rafal'kes, and P.A. Tesner, *Khimiya Tverdogo Topliva (Solid Fuel Chemistry)* **11**, 113 (1977).
18. P.A. Tesner, A.E. Gorodetskii, E.V. Denisevich, A.P. Zakhovov, and T.V. Tehunova, *Dokl. Akad. Nauk* **222**, 1384 (1975).
19. B.V. Derjaguin and D.V. Fedoseev, *Carbon* **11**, 299 (1973).
20. J. Warnatz in *Combustion Chemistry* (W.C. Gardiner, Ed.), Springer-Verlag, New York, 1984, p. 197.
21. D.B. Olson and W.C. Gardiner, *Combust. Flame* **32**, 151 (1978).
22. (a) J.E. Butler, J.W. Fleming, L.P. Goss, and M.C. Lin, in "Laser Probes for Combustion Chemistry," ACS Symposium Series **134**, 397 (1980). (b) P. Glarborg, J.A. Miller, and R.J. Kee, *Combust. Flame* **65**, 177 (1986).
23. W.J. Pitz and C.K. Westbrook, *Combust. Flame* **63**, 113 (1986).

Table I
Methane/Hydrogen mechanism

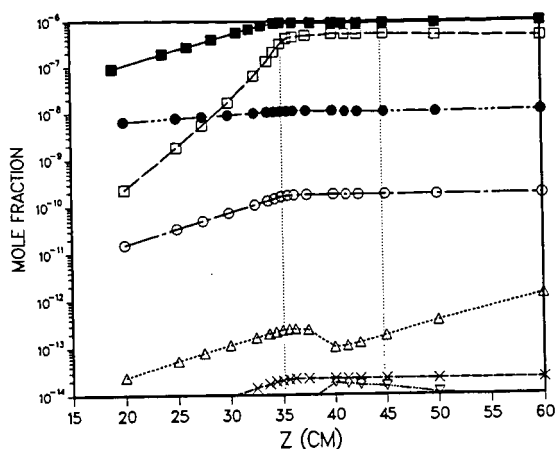
REACTIONS	A	n	E _a	Ref
A1) $H + H + M = H_2 + M$	9.7E+16	-0.6	0.0	20
A2) $CH_3 + H + M = CH_4 + M$	8.0E+26	-3.0	0.0	20 ^a
A3) $CH_4 + H = CH_3 + H_2$	2.2E+04	3.0	8.8	20
A4) $CH_4 + CH_2 = CH_3 + CH_3$	1.0E+13	0.0	0.0	21
A5) $CH_3 + CH_3 = C_2H_5 + H$	8.0E+14	0.0	26.5	20
A6) $CH_3 + H = CH_2 + H_2$	7.2E+14	0.0	15.1	21
A7) $CH_3 + CH_2 = C_2H_4 + H$	2.0E+13	0.0	0.0	21
A8) $CH_3 + M = CH_2 + H + M$	1.0E+16	0.0	90.6	20
A9) $CH_2 + H = CH + H_2$	4.0E+13	0.0	0.0	20
A10) $CH + CH_4 = C_2H_4 + H$	6.0E+13	0.0	0.0	22
A11) $CH + CH_3 = C_2H_3 + H$	3.0E+13	0.0	0.0	22
A12) $C_2H_6 + H = C_2H_5 + H_2$	5.4E+02	3.5	5.2	20 ^b
A13) $C_2H_6 + CH_3 = C_2H_5 + CH_4$	5.5E-01	4.0	8.3	20 ^b
A14) $C_2H_6 + M = CH_3 + CH_3 + M$	1.0E+19	0.0	68.0	20 ^b
A15) $C_2H_5 + M = C_2H_4 + H + M$	1.0E+17	0.0	31.0	20 ^b
A16) $C_2H_5 + CH_3 = C_2H_4 + CH_4$	7.9E+11	0.0	0.0	23
A17) $C_2H_4 + M = C_2H_2 + H_2 + M$	2.6E+17	0.0	79.4	20 ^b
A18) $C_2H_4 + M = C_2H_3 + H + M$	2.6E+17	0.0	96.6	20
A19) $C_2H_4 + H = C_2H_3 + H_2$	1.5E+14	0.0	10.2	20
A20) $C_2H_4 + CH_3 = CH_4 + C_2H_3$	4.2E+11	0.0	11.2	20
A21) $C_2H_3 + H = C_2H_2 + H_2$	2.0E+13	0.0	0.0	20
A22) $C_2H_3 + M = C_2H_2 + H + M$	3.0E+15	0.0	32.0	20
A23) $C_2H_3 + CH_3 = C_2H_2 + CH_4$	7.9E+11	0.0	0.0	23
A24) $C_2H_2 + M = C_2H + H + M$	4.0E+16	0.0	107.0	20
A25) $C_2H_2 + H = C_2H + H_2$	6.0E+13	0.0	23.7	20

$k = AT^n e^{-E_a/RT}$, $R = 1.99 \times 10^{-3}$ kcal/mole-deg

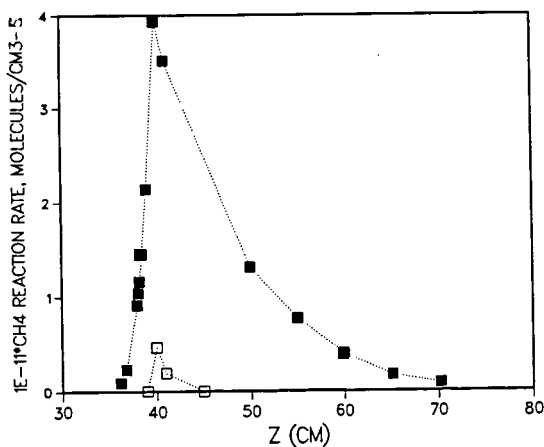
Units are cm³, moles, seconds, kilocalories

^a Results at $Z = 40$ are more sensitive to the value of this rate constant than to any other rate constant.

^b Results at $Z = 40$ show significant sensitivity to the value of this rate constant.



1. \log_{10} of mole fractions of all species calculated to have mole fractions of at least 10^{-14} . The vertical dotted lines indicate the location of the reaction chamber; the crucible holding the diamond seed crystals is at $Z = 40$ cm. Solid squares, C_2H_6 ; open squares, CH_3 ; solid circles, H ; open circles, C_2H_4 ; triangles, C_2H_5 ; crosses, C_2H_2 ; inverted triangles, CH_2 . CH_4 and H_2 , with mole fractions of 0.7 and 0.3, respectively, are not shown.



2. Molecules of CH_4 which reacted/ $cm^3 \cdot s$ as a function of Z . Solid squares, Reaction A_1 : $CH_4 + H \rightarrow CH_3 + H_2$. Open squares, Reaction A_{-2} : $CH_4 + M \rightarrow CH_3 + H + M$. For this analysis these reactions are considered only in the direction indicated by the arrows.